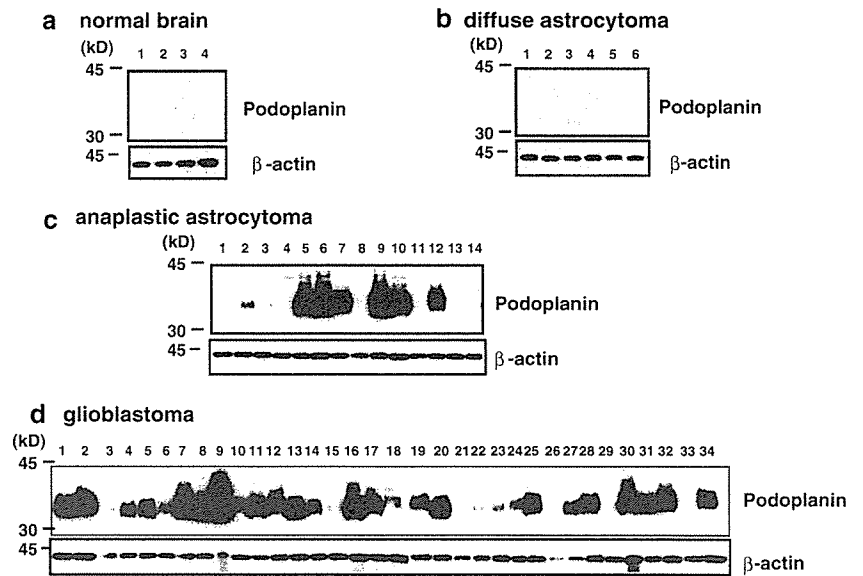**Fig. 2** Western blot analyses of podoplanin expression in astrocytic tumors. Tissues from normal brain (**a**), diffuse astrocytomas (**b**), anaplastic astrocytomas (**c**), and glioblastomas (**d**) were solubilized and immunoblotted using anti-human podoplanin monoclonal antibody YM-1 (*upper panel*) or anti-β-actin antibody (*lower panel*)

formation by promoting the rearrangement of the actin cytoskeleton [16]. PA2.26/podoplanin was identified as a cell surface protein induced in epidermal carcinogenesis and skin remodeling [18, 19]. Expression of PA2.26/ podoplanin in pre-malignant keratinocytes induces a fully transformed and metastatic phenotype. Furthermore, human PA2.26/podoplanin has been found in the

Fig. 3 Quantitative real-time PCR analysis of podoplanin transcripts in astrocytic tumors. First-strand cDNA samples derived from astrocytic tumor tissues of 54 patients (6 diffuse astrocytomas, 14 anaplastic astrocytomas, and 34 glioblastomas) and four normal brain tissues were used as real-time PCR templates. The respective expression levels of podoplanin were normalized to μg or total RNA, as described in Materials and methods

invasive front of oral squamous cell carcinomas, consistent with a role in tumor cell migration and invasion [12]. Moreover, a monoclonal antibody against gp44/aggrus/ podoplanin inhibits pulmonary metastasis of a highly metastatic clone of mouse colon adenocarcinoma in vivo [21, 22]. In this study, we showed upregulated expression of podoplanin in CNS malignant astrocytic tumors. Recently, Shibahara et al. [20] also reported podoplanin expression in subsets of CNS tumors. However, the results obtained so far showed only associations between podoplanin expression and malignancy of astrocytic tumors, while its direct biological function in malignant astrocytomas remains to be established.

PA2.26/podoplanin was co-localized with ezrin, radixin, moesin family proteins, which are concentrated in cell surface projections, where they link the actin cytoskeleton to plasma membrane proteins [18]. Consistent with the association of podoplanin with ezrin, the latter's immunoreactivity is also associated with increasing malignancy of astrocytic tumors [3, 23]. The combination of podoplanin and ezrin might thus represent a possible tool for grading of astrocytic tumors.

Platelets play an important role in hemostasis and thrombosis and are also involved in tissue repair and tumor metastasis [5]. Glioblastoma is differentiated from low-grade astrocytomas based on the histological presence of tumor necrosis and associated microvascular proliferation [11]. Large necroses are attributable to insufficient blood supply and thrombosed tumor vessels are often observed. We speculate that the local platelet aggregation and thrombus formation might be increased by podoplanin-expressing malignant astrocytic tumor cells, resulting in tumor vessel obstruction and subsequent necrosis. Indeed, our unpublished results suggest that podoplanin expressed by glioblastoma cells induces platelet aggregation in vitro (data not shown).
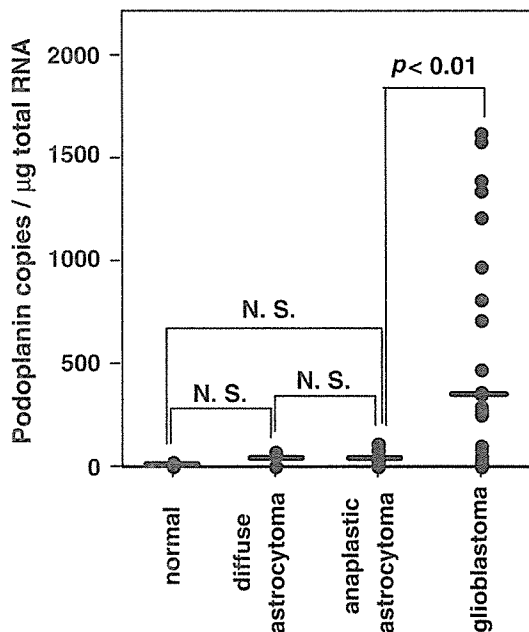
In conclusion, podoplanin expression was markedly higher in glioblastomas than in anaplastic astrocytomas. Furthermore, podoplanin expression was not observed in diffuse astrocytoma. It will be intriguing to investigate the functional basis of the association between podoplanin expression and malignant progression of astrocytomas.

References

1. Breiteneder-Geleff S, Soleiman A, Kowalski H, Horvat R, Amann G, Kriehuber E, Diem K, Weninger W, Tschachler E, Alitalo K, Kerjaschki D (1999) Angiosarcomas express mixed endothelial phenotypes of blood and lymphatic capillaries: podoplanin as a specific marker for lymphatic endothelium. Am J Pathol 154:385–394
2. DeAngelis LM (2001) Brain tumors. N Engl J Med 344:114–123
3. Geiger KD, Stoldt P, Schlote W, Derouiche A (2000) Ezrin immunoreactivity is associated with increasing malignancy of astrocytic tumors but is absent in oligodendrogliomas. Am J Pathol 157:1785–1793
4. Giese A, Bjerkvig R, Berens ME, Westphal M (2003) Cost of migration: invasion of malignant gliomas and implications for treatment. J Clin Oncol 21:1624–1636
5. Honn KV, Tang DG, Crissman JD (1992) Platelets and cancer metastasis: a causal relationship? Cancer Metastasis Rev 11:325–351
6. Kaneko M, Kato Y, Kunita A, Fujita N, Tsuruo T, Osawa M (2004) Functional sialylated O-glycan to platelet aggregation on Aggrus (T1alpha/podoplanin) molecules expressed in Chinese Hamster Ovary cells. J Biol Chem 279:38838–38843
7. Kato Y, Fujita N, Kunita A, Sato S, Kaneko M, Osawa M, Tsuruo T (2003) Molecular identification of Aggrus/T1alpha as a platelet aggregation-inducing factor expressed in colorectal tumors. J Biol Chem 278:51599–51605
8. Kato Y, Sasagawa I, Kaneko M, Osawa M, Fujita N, Tsuruo T (2004) Aggrus: a diagnostic marker that distinguishes seminoma from embryonal carcinoma in testicular germ cell tumors. Oncogene 23:8552–8556
9. Kato Y, Kaneko M, Sata M, Fujita N, Tsuruo T, Osawa M (2005) Enhanced expression of Aggrus (T1alpha/podoplanin), a platelet-aggregation-inducing factor in lung squamous cell carcinoma. Tumor Biol 26:195–200
10. Kleihues P, Ohgaki H (1999) Primary and secondary glioblastomas: from concept to clinical diagnosis. Neuro-oncology 1:44–51
11. Kleihues P, Burger PC, Collins VP, Newcomb EW, Ohgaki H, Cavenee WK (2000) Astrocytic tumors. Glioblastoma. In: Kleihues P, Cavenee WK (eds) Pathology and genetics of tumours of the nervous system. International Agency for Research on Cancer Press, Lyons, France, pp 29–39
12. Martin-Villar E, Scholl FG, Gamallo C, Yurrita MM, Munoz-Guerra M, Cruces J, Quintanilla M (2005) Characterization of human PA2.26 antigen (T1alpha-2, podoplanin), a small membrane mucin induced in oral squamous cell carcinomas. Int J Cancer 113:899–910
13. Mishima K, Kato Y, Kaneko KM, Nakazawa Y, Kunita A, Fujita N, Tsuruo T, Nishikawa R, Hirose T, Matsutani M (2006) Podoplanin expression in primary central nervous system germ cell tumors: a useful histological marker for the diagnosis of germinoma. Acta Neuropathol (Berl) (in press)
14. Ordonez NG (2005) D2-40 and podoplanin are highly specific and sensitive immunohistochemical markers of epithelioid malignant mesothelioma. Hum Pathol 36:372–380
15. Roy S, Chu A, Trojanowski JQ, Zhang PJ (2005) D2-40, a novel monoclonal antibody against the M2A antigen as a marker to distinguish hemangioblastomas from renal cell carcinomas. Acta Neuropathol (Berl) 109:497–502
16. Schacht V, Ramirez MI, Hong YK, Hirakawa S, Feng D, Harvey N, Williams M, Dvorak AM, Dvorak HF, Oliver G, Detmar M (2003) T1alpha/podoplanin deficiency disrupts normal lymphatic vasculature formation and causes lymphedema. EMBO J 22:3546–3556
17. Schacht V, Dadras SS, Johnson LA, Jackson DG, Hong YK, Detmar M (2005) Up-regulation of the lymphatic marker podoplanin, a mucin-type transmembrane glycoprotein, in human squamous cell carcinomas and germ cell tumors. Am J Pathol 166:913–921
18. Scholl FG, Gamallo C, Vilaro S, Quintanilla M (1999) Identification of PA2.26 antigen as a novel cell-surface mucin-type glycoprotein that induces plasma membrane extensions and increased motility in keratinocytes. J Cell Sci 112:4601–4613
19. Scholl FG, Gamallo C, Quintanilla M (2000) Ectopic expression of PA2.26 antigen in epidermal keratinocytes leads to destabilization of adherens junctions and malignant progression. Lab Invest 80:1749–1759
20. Shibahara J, Kashima T, Kikuchi Y, Kunita A, Fukayama M (2006) Podoplanin is expressed in subsets of tumors of the central nervous system. Virchows Arch (in press)
21. Sugimoto Y, Watanabe M, Oh-hara T, Sato S, Isoe T, Tsuruo T (1991) Suppression of experimental lung colonization of a metastatic variant of murine colon adenocarcinoma 26 by a monoclonal antibody 8F11 inhibiting tumor cell-induced platelet aggregation. Cancer Res 51:921–925
22. Tsuruo T, Yamori T, Naganuma K, Tsukagoshi S, Sakurai Y (1983) Characterization of metastatic clones derived from a metastatic variant of mouse colon adenocarcinoma 26. Cancer Res 43:5437–5442
23. Tynninen O, Carpen O, Jaaskelainen J, Paavonen T, Paetau A (2004) Ezrin expression in tissue microarray of primary and recurrent gliomas. Neuropathol Appl Neurobiol 30:472–477

Brain- and heart-specific *Patched-1* containing exon 12b is a dominant negative isoform and is expressed in medulloblastomas ☆

Hideki Uchikawa [a,b], Masashi Toyoda [a], Kazuaki Nagao [a], Hiroshi Miyauchi [c], Ryo Nishikawa [c], Katsunori Fujii [b], Yoichi Kohno [b], Masao Yamada [a], Toshiyuki Miyashita [a,*]

[a] *Department of Genetics, National Research Institute for Child Health and Development, Tokyo 157-8535, Japan*
[b] *Department of Pediatrics, Graduate School of Medicine, Chiba University, Chiba 260-8670, Japan*
[c] *Department of Neurosurgery, Saitama Medical School, Saitama 350-0495, Japan*

Abstract

Mutations in the human tumor suppressor gene, *Patched-1*, are associated with nevoid basal cell carcinoma syndrome characterized by developmental abnormalities and tumorigenesis, such as basal cell carcinoma and medulloblastoma. During the investigation of complex alternative splicing in *Patched-1*, we identified an alternative exon, exon 12b, located between exon 12 and 13, both in humans and in mice. Since exon 12b has an in-frame stop codon, the mRNA isoform containing this exon (*Patched12b*) encodes a truncated patched-1 protein. RT-PCR and whole mount *in situ* hybridization revealed that mouse exon 12b was expressed in the brain and heart, particularly in the cerebellum, in both adults and embryos. We next performed a functional analysis of *Patched12b* using a GLI-responsive luciferase reporter. Luciferase activity was suppressed when transfected with a plasmid encoding *Patched-1*, but not with a plasmid for *Patched12b*. The suppressive activity of Patched-1 was relieved when cotransfected with a plasmid for *Patched12b*. This implies that the Patched12b protein has a dominant negative effect on Patched-1. Interestingly, *Patched12b* was found to be expressed in some of the medulloblastoma tissues and cell lines, indicating an important role in the pathogenesis of medulloblastoma as well as brain development.
© 2006 Elsevier Inc. All rights reserved.

The *Patched-1* gene (*Ptc1*) controls cell growth and specification of the developing and postnatal tissues of many animals [1]. The nevoid basal cell carcinoma syndrome (NBCCS), also called Gorlin syndrome, is associated with mutations in a human *Ptc1* homolog, *PTCH* [2,3]. NBCCS is an autosomal dominant neurocutaneous disorder characterized by developmental malformations, such as syndac-

tyly and spina bifida, and an increased incidence of a variety of tumors, including basal cell carcinoma (BCC) and medulloblastoma [4]. Mutations of *PTCH* are also detected in a small fraction of holoprosencephaly characterized by a failure of the complete separation of the forebrain into right and left halves [5]. Heterozygous loss of *PTCH* found in certain sporadic and familial cases of BCC and medulloblastoma indicates that *PTCH* is also a tumor suppressor gene [6–8]. Ptc1, a 12-pass transmembrane protein, is the ligand-binding component of the receptor complex for a secreted protein, Sonic hedgehog (Shh). In the absence of Shh binding, Ptc1 is thought to hold Smoothened (Smo), another component of the Shh receptor, in an inactive state and thus inhibit signaling to

---

downstream genes. Upon the binding of Shh, the inhibition of Smo is released and signaling is transduced, leading to the activation of target genes by the Gli family of transcription factors [1].

We and others have identified a number of *PTCH* mRNA isoforms generated by alternative splicing (AS) [9–11]. Among these isoforms, the one containing exon 12b conserved in both humans and mice (*PTCH12b* and *Ptc12b*, respectively) is particularly interesting since it is expressed in a brain- and heart-specific fashion, at least in human tissues [12]. Here, we show that mouse *Ptc12b* is also preferentially expressed in the brain and in the heart. Since this isoform has an in-frame stop codon, it encodes truncated Ptc1, which does not seem to have any functions. However, the functional analysis of this isoform demonstrated that it functions as a dominant negative isoform against Ptc1. Furthermore, *PTCH12b* was found to be expressed in some of the medulloblastoma tissues and cell lines, indicating an important role in the pathogenesis of medulloblastomas as well as brain development.

Materials and methods

Constructs. The plasmids for myc-PTCH and 8 × GLI-Luc were kindly provided by Dr. J. Ming and Dr. S. Ishii, respectively. Mouse *Ptc1* cDNA sequence, exon 12-12b-13, was amplified by RT-PCR. The primers used for the amplification were 5′-TTCTCCCTCCAGTACTGATG-3′ (exon 12 forward), 5′-CACCACAGCAGCCTTGGGAG-3′ (exon 13 reverse). The PCR product was subcloned into pGEM-T Easy (Promega) and used for *in situ* hybridization. pMyc-PTCH and pMyc-PTCH12b were described previously [12]. To produce pPTCH-EGFP and pPTCH12b-EGFP, *PTCH* sequences for exon 1a-exon23 and exon 1a-exon12b, respectively, were amplified by PCR using pMyc-PTCHM or pMyc-PTCH12b as a template and subcloned into pEGFP-N3 (Clontech). The primers used for the amplification were 5′-GGGGTACCGCTATGGGGAAGGCTA CTGG-3′ (exon 1a-2 forward), 5′-CGGGATCCGTTGGAGCTGCTT CCCCGGG-3′ (exon 23 reverse), and 5′-CGGGATCCCTCCTCG TAAGGAAACCTCATGTA-3′ (exon 12b reverse). Restriction enzyme recognition sequences (underlined) were added to facilitate subcloning.

RT-PCR. Total RNA was extracted using the RNeasy kit from Qiagen according to the manufacturer's recommendations. RT-PCR was performed as previously described using 5 μg of total RNA [11]. Primers used for RT-PCR were 5′-TGGCCCATGCATTCAGTGAAACA-3′ (mouse exon 11 forward), 5′-GAGGGTCATACTCTGTGCGGA-3′ (mouse exon 14 reverse), 5′-GTGTTGGTGTGGATGATGTTT-3′ (human exon 11 forward), and 5′-CGGGATCCTTGTAAAACAGCAGAAAAT-3′ (human exon 13 reverse).

Western blotting. Immunoblot analysis was performed as described previously [13]. In brief, 30 μg of the cell lysate was subjected to SDS–PAGE and transferred onto a nitrocellulose membrane. The membrane was incubated with anti-c-Myc mouse monoclonal antibody (Santa Cruz, 9E10) followed by horseradish peroxidase-conjugated anti-mouse immunoglobulins (DAKO) or with anti-GFP rabbit polyclonal antibody (Medical & Biological Laboratories, Japan) followed by horseradish peroxidase-conjugated anti-rabbit IgG (Santa Cruz).

Luciferase assay. 1-23 cells growing on six-well plates were cotransfected using Effectene reagent (Qiagen) with various combinations of plasmids as indicated in Fig. 4. The total amount of transfected DNA was adjusted to 3 μg with an empty plasmid, pcDNA3.0. Twenty-four hours after the transfection, cells were harvested and subjected to the luciferase assay with the reagents and protocols provided by Promega. Firefly luciferase activity was nor-

malized by Renilla luciferase activity from a cotransfected pRL-SV40 (Promega).

In situ hybridization. The plasmids described above were linearized and digoxigenin-labeled cRNA probes were synthesized using T7 or SP6 RNA polymerase. E10.5 embryos on a C57BL/6J background were fixed in 4% paraformaldehyde in PBS, dehydrated in methanol, and stored at −20 °C. For hybridization, embryos were rehydrated in 0.1% Tween 20 in PBS (PBT) and incubated with proteinase K (10 μg/ml in PBT) for 15 min at 37 °C. Digestion was stopped by washing with 2 mg/ml glycine in PBT, and embryos were refixed in 4% paraformaldehyde and 0.25% glutaraldehyde in PBT, washed in PBT, and hybridized overnight at 65 °C with 2 μg/ml of digoxigenin-labeled RNA probes in hybridization solution (50% formamide, 5 × SSC, 2% blocking powder (Roche), 0.1% Tween 20, 0.5% CHAPS, 50 μg/ml yeast RNA, 5 mM EDTA, and 50 μg/ml heparin). Embryos were washed in hybridization solution and in 2 × SSC, 0.1% CHAPS at 65 °C, and incubated for 30 min with 20 μg/ml RNase A in 2 × SSC, 0.1% CHAPS at 37 °C. After washing, embryos were blocked for 3 h in 10% sheep serum, 1% BSA in PBT and incubated overnight at 4 °C with anti-digoxigenin antibody (Roche) (1:2000 diluted in 10% sheep serum, 1% BSA in PBT with 1.5 mg/ml mouse embryo powder). Embryos were washed 5 times in 1% BSA in PBT for 1 h each, 3 times in NTMT (100 mM NaCl, 100 mM Tris–HCl, pH 9.5, 50 mM MgCl$_2$, and 0.1% Tween 20) for 10 min each, and stained with NBT/BCIP stock solution (Roche) (1:50 diluted in NTMT) for about 2 h at room temperature.

Immunostaining and confocal microscopy. Immunostaining was performed essentially as described previously [14]. Briefly, HeLa cells were seeded on chamber slides (Nalge Nunc International) and were transfected with the constructs indicated in the figure legend. After 24 h, the slides were fixed with 4% paraformaldehyde, permeabilized, stained with anti-c-myc antibody (Santa Cruz, 9E10) followed with FITC-labeled anti-mouse immunoglobulins (DAKO), and observed with an Olympus microscope FV300. Nuclear localization was confirmed by Hoechst33342 staining. EGFP fusion proteins were observed as described previously [15].

Results

Tissue-specific regulation of Ptc12b expression in mice

Previously, we identified a *patched-1* isoform containing a novel exon, exon 12b, between exon 12 and exon 13 both in humans (*PTCH12b*) and in mice (*Ptc12b*) (GenBank Accession Nos. AB214500 and AB214501, respectively) [12]. Using RT-PCR and exon junction microarrays, *PTCH12b* was demonstrated to be expressed in a brain- and heart-specific fashion [12]. The nucleotide sequence of and adjacent to exon12b was relatively conserved in humans and in mice, especially around the 3′-end of the exon (Fig. 1A). Since premature termination codons (PTCs) were identified in both exons, they are expected to encode proteins truncated just after the sterol-sensing domain (Fig. 1B), whose function in PTCH remains elusive [16]. The splicing regulatory element, UGCAUG, reported to be phylogenetically and spatially conserved in introns that flank the brain-enriched alternative exons [17] was found in the intron regions upstream and downstream of exon 12b in both species (Fig. 1C), supporting the hypothesis that this element is a critical component for tissue-specific splicing events. We next investigated whether exon 12b was also preferentially

A 1 ctcctctcttagTACATACTGATGGCTCATCGAGGCCGACTCTCCT---TTAATGATACC
      *** * ** *****   ****** ***** **** *******   *** ** ** *
   1 ctctccactcagTAC----TGATGGTTCATCAAGGCAAACTCTCCTCCCTTATTGGTATC

  58 CTGTGGTGTGGTGGTCTGAAAAGCTAC-ATGAGGTTTCCTTACGAGGAGTAGCCTTGTAG
      * ******** **** *******   **** ***** * ***** ******* ***
  57 CCACGGTGTGGT-CTCTG-AAAGCTACGTTGAGTTTTCCCT--GAGGA-TAGCCTTTTAG

 117 AAAATCCAGTGCGCTAAATTCTCCCAAGgtaagcacctta
      ********** ****** ********************
 112 AAAATCCAGTACGCTAAGTTCTCCCAAGgtaagcacctta

B   1   SSD   1447
PTCH [▮   ▮▮▮▮▮   ▮   ▮▮▮▮▮   ]

                           607
PTCH12b [▮   ▮▮▮▮▮▮]

C   Exon 12   1 kb   Exon 12b   Exon 13
Human ▯┤   ▯   ▯
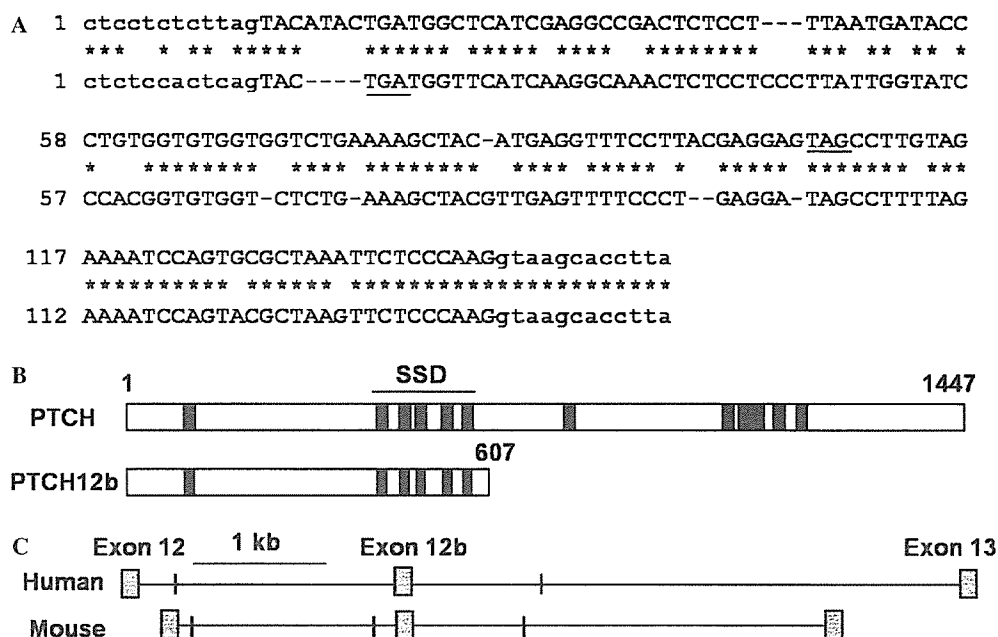Mouse ▯┤   ┤▯   ┤   ▯

Fig. 1. Exon 12b and flanking splicing elements are conserved in humans and in mice. (A) Alignment of human (upper) and murine (lower) exon 12b and surrounding sequences. Upper- and lowercase letters indicate the exon and intron sequences, respectively. Nucleotides are numbered arbitrarily. Conserved nucleotides are marked by asterisks. In-frame stop codons are underlined. (B) PTCH protein isoforms. Numbers refer to amino acid positions relative to the first methionine of PTCH (NM_000264). Transmembrane domains are indicated by filled boxes. The region containing the 2nd to 6th transmembrane domains comprises the sterol-sensing domain (SSD). (C) Location of UGCAUG hexamers near exon 12b. The location of hexamers is indicated by small vertical thick lines.

expressed in the mouse brain and heart. In adult mice, Ptc1 (12b−) was more or less expressed in various tissues. However, the Ptc12b isoform (12b+) was specifically expressed in the brain and in the heart, particularly in the cerebellum, but not in other tissues, such as the testis and the liver (Fig. 2A). To investigate the expression pattern in the mouse embryo, we performed whole mount in situ hybridization. Ptc12b was also expressed in the brain and in the heart (Fig. 2B), indicating some role yet to be identified in the development of these tissues. The specificity of the result was confirmed by the negative staining with the sense probe. Taken together, these results imply that the tissue-specific expression of this isoform is evolutionarily conserved.

PTCH12b is expressed in some medulloblastoma tissues and cell lines

Individuals with NBCCS are at high risk of medulloblastomas, which are primitive neuroectodermal tumors. Since medulloblastoma commonly arises in the cerebellum where *PTCH12b* is specifically expressed, we next addressed the question if this isoform is expressed in medulloblastoma cell lines and tissues. Out of 5 medulloblastoma cell lines analyzed, I-23 expressed very high level of *PTCH12b*. None of the 9 non-medulloblastoma cell lines expressed *PTCH12b*. Interestingly, it was also expressed in two out of two medulloblastoma tissues we examined, indicating that this isoform plays a role in the formation of medulloblastoma (Fig. 3A).
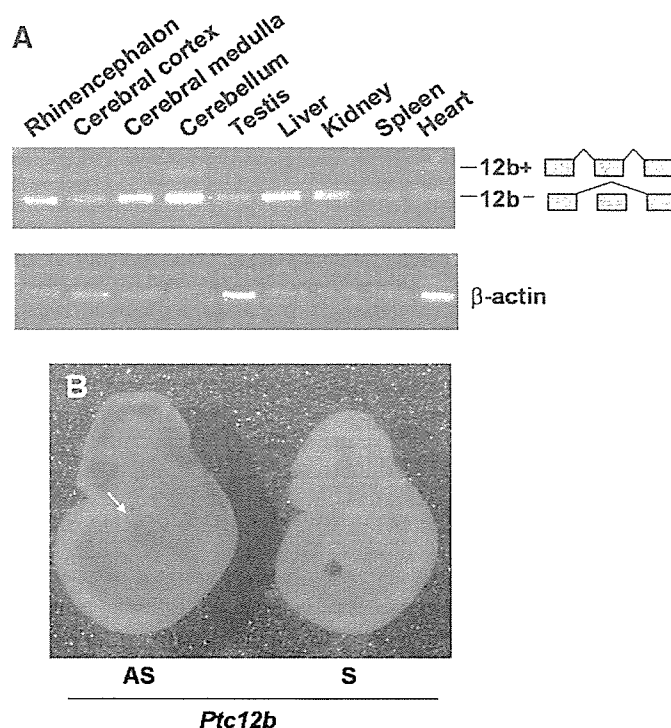

Fig. 2. Tissue-specific expression of *Ptc12b* in mice. (A) Total RNAs obtained from a panel of mouse tissues were subjected to RT-PCR with β-actin as an internal control. A forward primer for exon 11 and a reverse primer for exon 14 were synthesized and used for RT-PCR. All tissues were obtained from a 1-month-old mouse. (B) Whole mount in situ hybridization on mouse embryos. Digoxigenin-labeled RNA probes were synthesized in both orientations, sense (S) and antisense (AS), and used on embryos at E10.5. The arrow indicates the position of the heart.
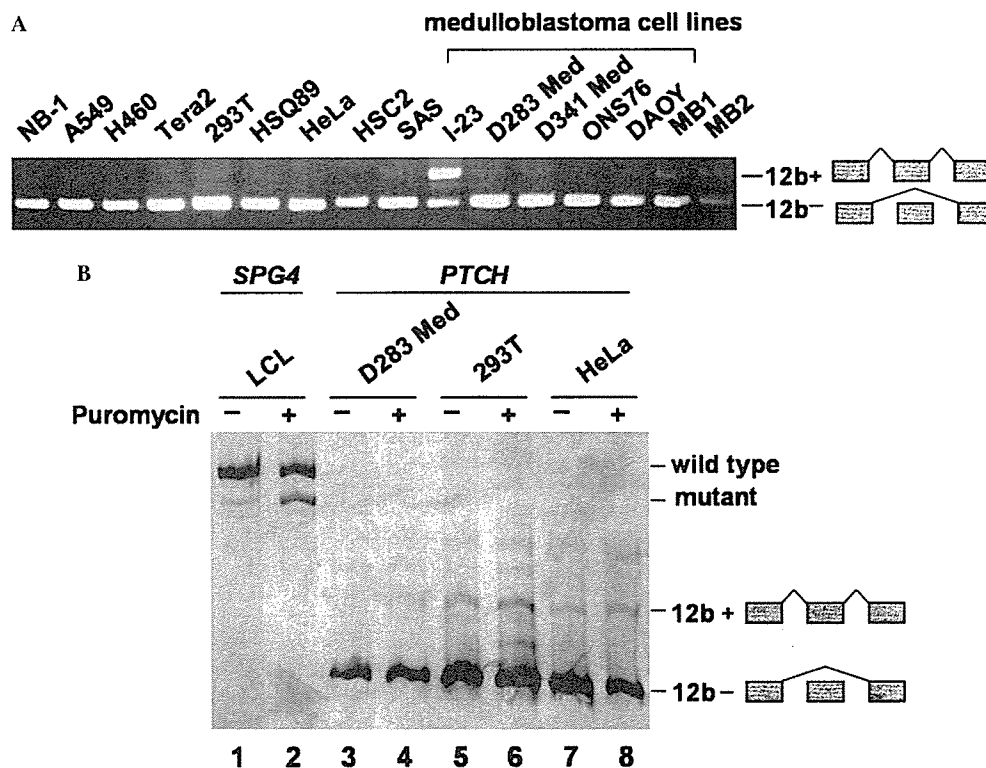
Fig. 3. Expression of exon12b in human cell lines and medulloblastomas. (A) RT-PCR analysis was performed using specific primers for exon 11 and exon 13. RNAs extracted from various cell lines and medulloblastoma samples (MB1, MB2) were used as templates. (B) *PTCH12b* is subjected to NMD to a small extent. Cell lines indicated at the top were grown in the presence or absence of 100 μg/ml puromycin for 6 h. Total RNA was extracted and subjected to RT-PCR. The RT-PCR products were run on a 3.5% polyacrylamide gel to emphasize the difference in size between transcripts from wild type allele and mutant allele of the *SPG4* gene.

PTCH12b isoform undergoes NMD to a small extent

It is known that spliced transcripts with PTCs, such as *Ptc12b* or *PTCH12b*, can potentially activate transcript degradation via the process of nonsense-mediated mRNA decay (NMD) [18]. NMD is important for the removal of PTC-containing transcripts encoding nonfunctional or potentially dominant negative proteins. In order to investigate this possibility, D283 Med, 293T, and HeLa cells, which express barely detectable levels of *PTCH12b*, were cultured in the presence or absence of an NMD inhibitor, puromycin, and subjected to RT-PCR as described above. A lymphoblastoid cell line (LCL) established from a patient in which a PTC is created due to the mutation in the *SPG4* gene (unpublished data by H. U., K. F. and T. M.) was employed as a positive control for NMD. Compared with the positive control where the levels of the transcript containing PTC were markedly increased upon the treatment with puromycin (Fig. 3B, lane 2, mutant), the transcripts of *PTCH12b* were only marginally elevated upon the treatment (Fig. 3B, lanes 4, 6, and 8). Similar results were obtained using another NMD inhibitor, cycloheximide (data not shown). This implies that this isoform undergoes NMD to a limited extent and is already expressed at low abundance independently of NMD in most tissues.

PTCH12b functions as a dominant negative isoform

We performed a functional analysis of PTCH12b using a GLI-responsive luciferase reporter in I-23 medulloblastoma cells. The binding of Shh to its receptor activates a signaling cascade that ultimately leads to an increased activity of the GLI family of transcription factors. The luciferase activities were suppressed when I-23 cells were transfected with plasmids for PTCH, but not with a plasmid for PTCH12b, consistent with PTCH being a suppressive component of the Shh receptor. This also implies that there is a basal level of leakage activity of Smo that excess PTCH prevents in the apparent absence of Shh. However, this suppression by PTCH was relieved when cotransfected with a plasmid for PTCH12b (Fig. 4A). Taken together, these results imply that the PTCH12b protein has a dominant negative effect on PTCH. In order to investigate the subcellular localizations, PTCH12b, as well as PTCH, both tagged with myc at their N-terminal ends, was expressed in HeLa cells and stained with an anti-myc antibody followed by confocal microscopy. PTCH was mainly localized in cytoplasmic vesicular structures as previously reported [19], and no significant difference in localization was observed between PTCH and PTCH12b (Fig. 4B and C). Therefore, it is unlikely that the dominant negative function of PTCH12b is due to its subcellular localization dis-
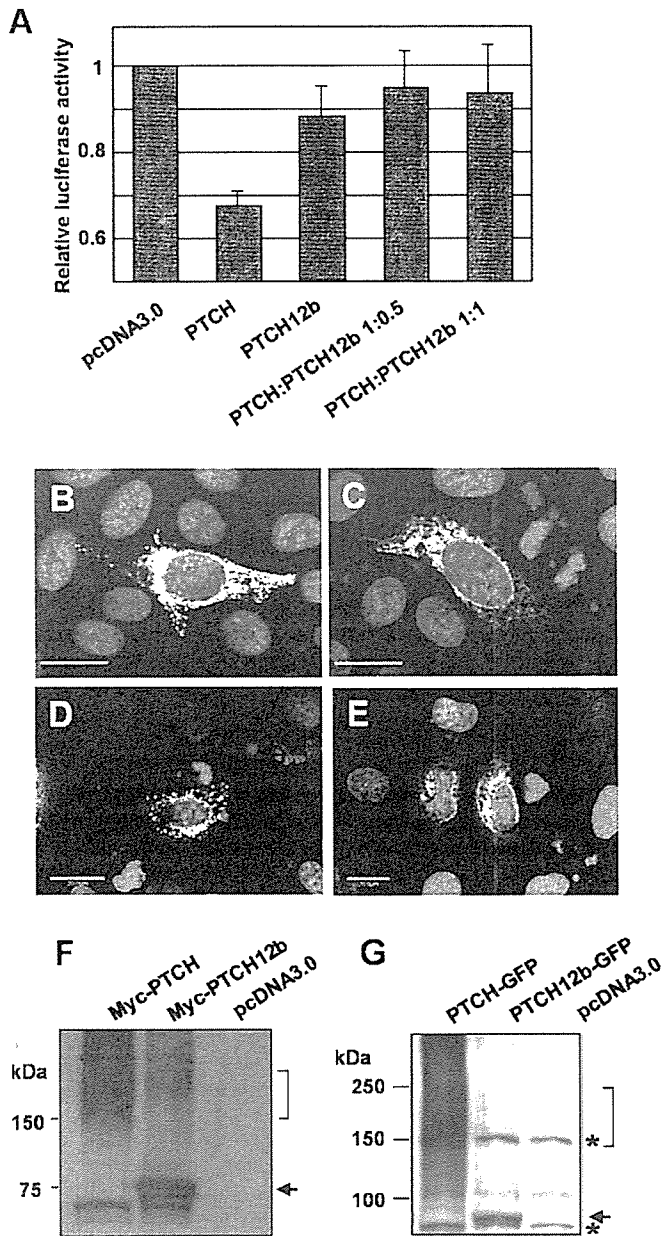
Fig. 4. Functional analysis of *PTCH12b*. (A) I-23 cells were transfected with various combinations of expression plasmids indicated at the bottom, together with a construct for a GLI-responsive luciferase reporter, 8 × GLI-Luc. Twenty-four hours after the transfection, cells were harvested and subjected to a luciferase assay. Shown are the representative data obtained in two independent experiments with triplicates in each experiment. (B–E) Subcellular localization of PTCH proteins. The expression patterns of myc-tagged (B and C) and EGFP-tagged (D and E) PTCH (B and D) or PTCH12b (C and E) in HeLa cells were examined using confocal microscopy. The nuclei were counterstained with Hoechst33342. Bar, 20 μm. (F and G) Western blotting was performed using protein samples obtained from the HeLa cells described above. Anti-c-myc (F) and anti-GFP (G) antibodies were used as a primary antibody. Asterisks indicate non-specific bands.

tinct from PTCH. Similar results were obtained when the both isoforms tagged with enhanced green fluorescent protein (EGFP) at their C-terminal ends were expressed (Fig. 4D and E). Comparative levels of protein expressions

of both PTCH and PTCH12b with expected sizes were confirmed by Western blotting (Fig. 4F and G), indicating that the stability of the PTCH12b protein is similar to that of PTCH.

Discussion

Exon 12b in the human *PTCH* gene is conserved in mice and expressed in a brain- and heart-specific manner in both species. According to a recent report by Pan et al., alternative exons with the potential to introduce PTCs upon exon inclusion are not usually conserved between humans and mice [20], suggesting some biological significance of exon 12b.

The precise mechanism of how Ptc12b/PTCH12b functions as a dominant negative isoform remains to be elucidated. Recently, two mutant forms of the Ptc1 protein, G509V and 1130X, have been reported to be dominant negative forms, at least in *Drosophila* [21–23]. Whereas 1130X accumulated strongly along the plasma membrane, G509V and wild type Ptc1 protein localized mainly in the cytoplasmic vesicles, indicating that their mode of action is different [22,23]. Our isoform localized in the cytoplasm. We failed to detect a significant difference in the subcellular localization between PTCH and PTCH12b. It would be interesting to see the *in vivo* function of Ptc12b/PTCH12b using animal models.

The important question would be whether truncated PTCH proteins generally function in a dominant negative manner, because most of the mutations found in patients with NBCCS lead to the truncation of the PTCH protein due to the frameshift or nonsense mutations [24,25]. $Ptc1^{-/-}$ mice are embryonic lethal due to the failure of neural tube closure and abnormal development of the heart [26]. Therefore, if truncated PTCH proteins are generally dominant negatives, then the patients with NBCCS should have a phenotype similar to that of $Ptc1^{-/-}$ mice, which is not the case. There are at least three explanations regarding this issue. First, mRNA with a frameshift or nonsense mutation may be expressed less than the wild type through NMD-dependent and/or independent mechanisms [20]. Second, at least truncated proteins with a large C-terminal deletion are unlikely to function as a dominant negative. Third, the sensitivity to the perturbation of SHH signaling may be species dependent. For example, mutations in the *SHH* gene are found in some of the children with autosomal dominant holoprosencephaly [27,28], whereas a phenotype resembling human holoprosencephaly is found in $Shh^{-/-}$ mice, but not in $Shh^{+/-}$ mice [29].

Synthesis of large amounts of C-terminally truncated polypeptides encoded by PTC-containing mRNA is avoided by a splicing- and translation-dependent NMD. Therefore, we wondered why *Ptc12b/PTCH12b* is expressed at high levels in certain tissues. Since NMD inhibition resulted in a limited amount of increase in expression of *PTCH12b*, we concluded that this isoform is already present at low levels independently from NMD in most tissues,

and that in the brain and some of the medulloblastomas it is abundantly expressed through a mechanism distinct from the inhibition of NMD. This conclusion is not surprising considering the recent report that only a fraction of PTC-introducing AS events are significantly regulated by NMD [20].

Although a relatively low frequency (10–20%) of sporadic medulloblastomas carry *PTCH* mutations [8], microarray analysis revealed that almost all medulloblastomas with desmoplastic histology are characterized by activation of the SHH signaling pathway [30]. Given the dominant negative function of PTCH12b and the detection of this isoform in the cerebellum and medulloblastoma, it is intriguing to speculate that *PTCH12b* plays an important role in the development of medulloblastoma. In our experiment, 1 out of 5 medulloblastoma cell lines expressed this isoform, whereas 2 out of 2 medulloblastoma tissues expressed this isoform. This may reflect the recent report that Shh activity is down-regulated in cultured medulloblastoma cells [31]. Tumor-specific AS is not a rare event based on a genome-wide computational screen [32]. However, the functional significance of respective protein isoforms generated by these ASs in oncogenesis has yet to be clarified. In NBCCS patients, 65 out of 132 *PTCH* mutations (49%) are localized in the second half of the protein (exon 13 or more downstream). Interestingly, in sporadic medulloblastomas, 16 out of 23 mutations (70%) are found in this region [33], implying that the gene structure encoding *PTCH12b* is more frequently preserved in sporadic medulloblastomas. Although more cases are needed to be investigated, consideration of not only the total expression levels of *PTCH* but also the expression of this particular *PTCH* isoform may help classify medulloblastomas and predict the clinical outcome of the children with medulloblastoma. Lastly, it should be noted that 3% of the individuals with NBCCS are known to have cardiac fibromas [34] and the heart is another tissue where *PTCH12b* is expressed.

Acknowledgments

References

[1] P.W. Ingham, A.P. McMahon, Hedgehog signaling in animal development: paradigms and principles, Genes Dev. 15 (2001) 3059–3087.

[2] R.L. Johnson, A.L. Rothman, J. Xie, L.V. Goodrich, J.W. Bare, J.M. Bonifas, A.G. Quinn, R.M. Myers, D.R. Cox, E.H. Epstein Jr., M.P. Scott, Human homolog of *patched*, a candidate gene for the basal cell nevus syndrome, Science 272 (1996) 1668–1671.

[3] H. Hahn, C. Wicking, P.G. Zaphiropoulous, M.R. Gailani, S. Shanley, A. Chidambaram, I. Vorechovsky, E. Holmberg, A.B. Unden, S. Gillies, K. Negus, I. Smyth, C. Pressman, D.J. Leffell, B. Gerrard, A.M. Goldstein, M. Dean, R. Toftgard, G. Chenevix-Trench, B. Wainwright, A.E. Bale, Mutations of the human homolog of *Drosophila patched* in the nevoid basal cell carcinoma syndrome, Cell 85 (1996) 841–851.

[4] R.J. Gorlin, Nevoid basal-cell carcinoma syndrome, Medicine (Baltimore) 66 (1987) 98–113.

[5] J.E. Ming, M.E. Kaupas, E. Roessler, H.G. Brunner, M. Golabi, M. Tekin, R.F. Stratton, E. Sujansky, S.J. Bale, M. Muenke, Mutations in PATCHED-1, the receptor for SONIC HEDGEHOG, are associated with holoprosencephaly, Hum. Genet. 110 (2002) 297–301.

[6] M.R. Gailani, M. Stahle-Backdahl, D.J. Leffell, M. Glynn, P.G. Zaphiropoulos, C. Pressman, A.B. Undén, M. Dean, D.E. Brash, A.E. Bale, R. Toftgård, The role of the human homologue of *Drosophila patched* in sporadic basal cell carcinomas, Nat. Genet. 14 (1996) 78–81.

[7] A.B. Undén, E. Holmberg, B. Lundh-Rozell, M. Stahle-Backdahl, P.G. Zaphiropoulos, R. Toftgård, I. Vorechovsky, Mutations in the human homologue of *Drosophila patched* (*PTCH*) in basal cell carcinomas and the Gorlin syndrome: different in vivo mechanisms of PTCH inactivation, Cancer Res. 56 (1996) 4562–4565.

[8] C. Raffel, R.B. Jenkins, L. Frederick, D. Hebrink, B. Alderete, D.W. Fults, C.D. James, Sporadic medulloblastomas contain *PTCH* mutations, Cancer Res. 57 (1997) 842–845.

[9] P. Kogerman, D. Krause, F. Rahnama, L. Kogerman, A.B. Undén, P.G. Zaphiropoulos, R. Toftgård, Alternative first exons of *PTCH1* are differentially regulated *in vivo* and may confer different functions to the PTCH1 protein, Oncogene 21 (2002) 6007–6016.

[10] T. Shimokawa, F. Rahnama, P.G. Zaphiropoulos, A novel first exon of the *Patched1* gene is upregulated by Hedgehog signaling resulting in a protein with pathway inhibitory functions, FEBS Lett. 578 (2004) 157–162.

[11] K. Nagao, M. Toyoda, K. Takeuchi-Inoue, K. Fujii, M. Yamada, T. Miyashita, Identification and characterization of multiple isoforms of a murine and human tumor suppressor, *patched*, having distinct first exons, Genomics 85 (2005) 462–471.

[12] K. Nagao, N. Togawa, K. Fujii, H. Uchikawa, Y. Kohno, M. Yamada, T. Miyashita, Detecting tissue-specific alternative splicing and disease-associated aberrant splicing of the *PTCH* gene with exon junction microarrays, Hum. Mol. Genet. 14 (2005) 3379–3388.

[13] T. Miyashita, Y. Okamura-Oho, Y. Mito, S. Nagafuchi, M. Yamada, Dentatorubral pallidoluysian atrophy (DRPLA) protein is cleaved by caspase-3 during apoptosis, J. Biol. Chem. 272 (1997) 29238–29242.

[14] M. U, T. Miyashita, Y. Ohtsuka, Y. Okamura-Oho, Y. Shikama, M. Yamada, Extended polyglutamine selectively interacts with caspase-8 and -10 in nuclear aggregates, Cell Death Differ. 8 (2001) 377–386.

[15] Y. Shikama, M. U, T. Miyashita, M. Yamada, Comprehensive studies on subcellular localizations and cell death-inducing activities of eight GFP-tagged apoptosis-related caspases, Exp. Cell Res. 264 (2001) 315–325.

[16] P.E. Kuwabara, M. Labouesse, The sterol-sensing domain: multiple families, a unique role? Trends Genet. 18 (2002) 193–201.

[17] S. Minovitsky, S.L. Gee, S. Schokrpur, I. Dubchak, J.G. Conboy, The splicing regulatory element, UGCAUG, is phylogenetically and spatially conserved in introns that flank tissue-specific alternative exons, Nucleic Acids Res. 33 (2005) 714–724.

[18] J.A. Holbrook, G. Neu-Yilik, M.W. Hentze, A.E. Kulozik, Nonsense-mediated decay approaches the clinic, Nat. Genet. 36 (2004) 801–808.

[19] J. Taipale, M.K. Cooper, T. Maiti, P.A. Beachy, Patched acts catalytically to suppress the activity of Smoothened, Nature 418 (2002) 892–896.

[20] Q. Pan, A.L. Saltzman, Y.K. Kim, C. Misquitta, O. Shai, L.E. Maquat, B.J. Frey, B.J. Blencowe, Quantitative microarray profiling provides evidence against widespread coupling of alternative splicing

with nonsense-mediated mRNA decay to control gene expression, Genes Dev. 20 (2006) 153–158.

[21] R.L. Johnson, L. Milenkovic, M.P. Scott, In vivo functions of the patched protein: requirement of the C terminus for target gene inactivation but not Hedgehog sequestration, Mol. Cell 6 (2000) 467–478.

[22] A.J. Zhu, L. Zheng, K. Suyama, M.P. Scott, Altered localization of *Drosophila* Smoothened protein activates Hedgehog signal transduction, Genes Dev. 17 (2003) 1240–1252.

[23] G.R. Hime, H. Lada, M.J. Fietz, S. Gillies, A. Passmore, C. Wicking, B.J. Wainwright, Functional analysis in *Drosophila* indicates that the NBCCS/PTCH1 mutation G509V results in activation of smoothened through a dominant-negative mechanism, Dev. Dyn. 229 (2004) 780–790.

[24] C. Wicking, S. Shanley, I. Smyth, S. Gillies, K. Negus, S. Graham, G. Suthers, N. Haites, M. Edwards, B. Wainwright, G. Chenevix-Trench, Most germ-line mutations in the nevoid basal cell carcinoma syndrome lead to a premature termination of the PATCHED protein, and no genotype-phenotype correlations are evident, Am. J. Hum. Genet. 60 (1997) 21–26.

[25] K. Fujii, Y. Kohno, K. Sugita, M. Nakamura, Y. Moroi, K. Urabe, M. Furue, M. Yamada, T. Miyashita, Mutations in the human homologue of *Drosophila patched* in Japanese nevoid basal cell carcinoma syndrome patients, Hum. Mutat. 21 (2003) 451–452.

[26] L.V. Goodrich, L. Milenković, K.M. Higgins, M.P. Scott, Altered neural cell fates and medulloblastoma in mouse patched mutants, Science 277 (1997) 1109–1113.

[27] E. Belloni, M. Muenke, E. Roessler, G. Traverso, J. Siegel-Bartelt, A. Frumkin, H.F. Mitchell, H. Donis-Keller, C. Helms, A.V. Hing, H.H. Heng, B. Koop, D. Martindale, J.M. Rommens, L.C. Tsui, S.W. Scherer, Identification of Sonic hedgehog as a candidate gene responsible for holoprosencephaly, Nat. Genet. 14 (1996) 353–356.

[28] E. Roessler, E. Belloni, K. Gaudenz, P. Jay, P. Berta, S.W. Scherer, L.C. Tsui, M. Muenke, Mutations in the human Sonic Hedgehog gene cause holoprosencephaly, Nat. Genet. 14 (1996) 357–360.

[29] C. Chiang, Y. Litingtung, E. Lee, K.E. Young, J.L. Corden, H. Westphal, P.A. Beachy, Cyclopia and defective axial patterning in mice lacking Sonic hedgehog gene function, Nature 383 (1996) 407–413.

[30] S.L. Pomeroy, P. Tamayo, M. Gaasenbeek, L.M. Sturla, M. Angelo, M.E. McLaughlin, J.Y. Kim, L.C. Goumnerova, P.M. Black, C. Lau, J.C. Allen, D. Zagzag, J.M. Olson, T. Curran, C. Wetmore, J.A. Biegel, T. Poggio, S. Mukherjee, R. Rifkin, A. Califano, G. Stolovitzky, D.N. Louis, J.P. Mesirov, E.S. Lander, T.R. Golub, Prediction of central nervous system embryonal tumour outcome based on gene expression, Nature 415 (2002) 436–442.

[31] K. Sasai, J.T. Romer, Y. Lee, D. Finkelstein, C. Fuller, P.J. McKinnon, T. Curran, Shh pathway activity is down-regulated in cultured medulloblastoma cells: implications for preclinical studies, Cancer Res. 66 (2006) 4215–4222.

[32] Z. Wang, H.S. Lo, H. Yang, S. Gere, Y. Hu, K.H. Buetow, M.P. Lee, Computational analysis and experimental validation of tumor-associated alternative RNA splicing in human cancer, Cancer Res. 63 (2003) 655–657.

[33] E. Lindström, T. Shimokawa, R. Toftgård, P.G. Zaphiropoulos, PTCH mutations: distribution and analyses, Hum. Mutat. 27 (2006) 215–219.

[34] D.G. Evans, E.J. Ladusans, S. Rimmer, L.D. Burnell, N. Thakker, P.A. Farndon, Complications of the naevoid basal cell carcinoma syndrome: results of a population based study, J. Med. Genet. 30 (1993) 460–464.

ORIGINAL PAPER

Kazuhiko Mishima · Yukinari Kato · Mika K. Kaneko
Youya Nakazawa · Akiko Kunita · Naoya Fujita
Takashi Tsuruo · Ryo Nishikawa · Takanori Hirose
Masao Matsutani

Podoplanin expression in primary central nervous system germ cell tumors: a useful histological marker for the diagnosis of germinoma

Abstract Podoplanin, a mucin-like transmembrane sialoglycoprotein, promotes platelet aggregation and may be involved in cancer cell migration, invasion, metastasis, and malignant progression. Podoplanin/aggrus is highly expressed in testicular seminoma, suggesting that it may be a sensitive marker for testicular seminomas. Here we investigated the expression of podoplanin in central nervous system (CNS) germ cell tumors (GCTs) by immunohistochemical staining of tumor samples from 62 patients. In 40 of 41 (98%) germinomas (including germinomatous components in mixed GCTs), podoplanin was diffusely expressed on the surface of germinoma cells; lymphocytes, interstitial cells, and syncytiotrophoblastic giant cells were negative for podoplanin. Except for immature teratomas (12/17; 71%), podoplanin expression was absent in non-ger-minomatous GCTs, including seven teratomas, seven embryonal carcinomas, seven yolk sac tumors, and seven choriocarcinomas. In immature teratomas, focal podoplanin staining was observed in fewer than 10% of immature squamous and columnar epithelial cells. Thus, podoplanin expression may be a sensitive immunohistochemical marker for germinoma in CNS GCTs. As such, it may be useful for diagnosis, for monitoring the efficacy of treatment, and as a potential target for antibody-based therapy.

Kazuhiko Mishima and Yukinari Kato contributed equally to this work.

Y. Kato (✉) · Y. Nakazawa · A. Kunita · N. Fujita · T. Tsuruo
Institute of Molecular and Cellular Biosciences,
The University of Tokyo, 1-1-1, Yayoi, Bunkyo-ku,
113-0032 Tokyo, Japan
E-mail: yukinari-k@bea.hi-ho.ne.jp
Tel.: +81-3-5841-7863
Fax: +81-3-5841-8487

K. Mishima · R. Nishikawa · M. Matsutani
Department of Neurosurgery, Saitama Medical School,
38 Morohongo, Moroyama-machi, Iruma-gun,
350-0495 Saitama, Japan

M. K. Kaneko
Department of Developmental Neuroscience,
Tokyo Metropolitan Institute for Neuroscience,
2-6, Musashidai, Fuchu, 183-8526 Tokyo, Japan

T. Tsuruo
Cancer Chemotherapy Center, Japanese Foundation for Cancer
Research, 3-10-6, Ariake, Koto-Ku, 135-8550 Tokyo, Japan

T. Hirose
Department of Pathology, Saitama Medical School,
38 Morohongo, Moroyama-machi, Iruma-gun,
350-0495 Saitama, Japan

Introduction

Germ cell tumors (GCTs) of the central nervous system (CNS) are a heterogeneous group of lesions found in children and young adults. They are classified into five basic histological types—germinoma, teratoma, embryonal carcinoma, yolk sac tumor, and choriocarcinoma—and into mixed tumor types when two or more components are present [14]. The prognosis of GCTs, independent of their location in the CNS, is highly dependent on the histological subtype. In general, germinomas are sensitive to radiotherapy and chemotherapy and have a better prognosis than non-germinomatous GCTs containing highly malignant components (e.g., embryonal carcinoma, yolk sac tumor, or choriocarcinoma). The 5-year survival rates are 95.4 and 17.4%, respectively [11].

Tumor markers can be helpful in diagnosing GCTs and assessing prognosis. Alpha-fetoprotein (AFP) is produced by yolk sac tumors, a part of embryonal carcinomas and immature teratomas, and beta human chorionic gonadotropin (HCG) is produced by syncytiotrophoblasts in choriocarcinomas. Embryonal carcinomas often have both of these components and therefore are associated with both markers [21]. Human placental alkaline phosphatase (PLAP), expressed by

primodial germ cells, has been widely used for immu-nochemical diagnosis of germinomas. However, it lacks specificity and its low secretion titer makes detection difficult [21]. Immunohistochemical staining after tumor resection is often important for diagnosis, and the dif-ferentiation between germinoma and non-germinoma-tous GCTs is essential for determining the appropriate treatment of CNS GCTs.

Mouse podoplanin (aggrus), a 44-kDa sialoglyco-protein with platelet aggregation-inducing ability, is expressed on the surface of mouse colon adenocarci-noma cells [22]. Antibody against podoplanin inhibited lung metastasis of NL-17 colon carcinoma cells in vivo. [20]. Cloning of cDNA revealed that human podoplanin is identical to T1α, a separately isolated protein that can also induce mouse and human platelet aggregation [5]. Therefore, podoplanin could be involved in platelet aggregation induced by tumor cells and metastasis. Po-doplanin expression was found in lymphatic endothe-lium and in tumor-associated lymphangiogenesis, and podoplanin deficiency resulted in congenital lymphe-dema and impaired lymphatic vascular patterning [16]. Furthermore, podoplanin expression has been shown to be upregulated in squamous cell carcinomas, testicular seminomas, and several sarcomas [2, 6, 7, 17].

Recently, Schacht et al. [17] showed that antibody D2-40, originally produced against a glycoprotein named oncofetal M2A antigen, specifically recognizes human podoplanin. They also demonstrated strong expression of podoplanin by ovarian dysgerminomas. D2-40 reacts with fetal gonocytes, testicular seminoma, and dysgerminoma [9]. Roy et al. [15] reported that D2-40 is a useful marker to distinguish hemangioblastoma from metastatic renal cell carcinoma in the brain. In the adult non-neoplastic CNS, D2-40 staining was seen in the subependymal areas, the leptomeninges and Purkinje cells.

In this study, we investigated the expression of po-doplanin in primary GCTs of the CNS to evaluate its potential as a diagnostic marker for CNS germinomas.

Materials and methods

Tissue samples

Tumors specimens were obtained at surgery from 62 patients with GCTs of the CNS, ten patients with CNS lymphomas, three patients with central neurocytoma, three patients with pineocytoma, three patients with pineoblastoma, three patients with schwannoma, four patients with meningioma, seven patients with meta-static brain tumors from lung cancer, three from breast cancer, one from colorectal cancer, and two from renal cell carcinoma. There were 27 germinomas, two germi-nomas with syncytiotrophoblastic giant cells (STGCs), three embryonal carcinomas, three yolk sac tumors, two choriocarcinomas, nine immature teratomas, four ter-atomas, and 12 mixed tumors (Table 1). Hematoxylin-and eosin-stained slides from these cases were reevalu-ated to confirm the diagnosis, and the tumors were categorized according to World Health Organization criteria [14]. Informed consent was obtained from all patients.

Antibodies

Anti-human podoplanin (aggrus) monoclonal antibody (YM-1: Medical Biological Laboratories, Nagoya, Ja-pan) was obtained by immunizing rats with the synthetic peptide CEGGVAMPGAEDDVV, corresponding to amino acids 38–51 of human podoplanin plus the N-terminal cysteine [4].

Table 1 Results of podoplanin immunostaining in 62 patients with GCTs

Tumor type	No. of cases	Podoplanin immunostaining				Positive cells
		+++	++	+	−	
Pure GCTs						
Germinoma	27	25	0	1	1	Germinoma cells
Germinoma with STGCs	2	2	0	0	0	Germinoma cells
Non-germinomatous GCTs						
Embryonal carcinoma	3	0	0	0	3	
Yolk sac tumor	3	0	0	0	3	
Choriocarcinoma	2	0	0	0	2	
Immature teratoma	9	0	0	4	5	Squamous and columnar epithelial cells
Teratoma	4	0	0	0	4	
Mixed GCTs						
Germinoma and teratoma	3	3	0	0	0	Germinoma component
Germinoma and choriocarcinoma	1	1	0	0	0	Germinoma component
Immature teratoma, yolk sac tumor, embryonal carcinoma, choriocarcinoma, and germinoma	4	0	0	4	0	Germinoma and immature teratoma
Immature teratoma and germinoma	4	0	0	4	0	Germinoma and immature teratoma

Western blot analysis

The tissues were solubilized with lysis buffer [25 mM Tris (pH 7.4), 50 mM NaCl, 0.5% Na deoxycholate, 2% Nonidet P-40, 0.2% SDS, 1 mM phenylmethylsulfonyl fluoride, and 50 mg/ml aprotinin] and electrophoresed under reducing conditions on 10–20% polyacrylamide gels (DRC, Tokyo, Japan). The separated proteins were transferred to a nitrocellulose membrane. After blocking with 4% skim milk in PBS, the membrane was incubated first with YM-1 or anti-β-actin antibody (Sigma, St. Louis, MO, USA), and then with peroxidase-conjugated secondary antibodies (Amersham, Buckinghamshire, UK) and developed for 3 min with ECL reagents (Amersham) using Kodak X-Omat AR film.

Immunohistochemistry

For immunohistochemical analysis, specimens were deparaffinized, rehydrated, and incubated first with YM-1 (1:20 dilution of concentrated culture supernatant from Medical Biological Laboratories) at room temperature for 1 h, then with biotin-conjugated secondary anti-rat IgG antibody (DakoCytomation, Glostrup, Denmark) for 1 h, and finally with peroxidase-conjugated avidin-streptavidin complex (Vectastain ABC Kit, Vector Laboratories, Peterborough, UK) for 1 h. Color was developed with 3, 3-diaminobenzidine tetrahydrochloride tablet sets (DakoCytomation) for 3 min. Immunohistochemical staining for tumor markers including beta-HCG, AFP, and PLAP was also used to confirm the classification. Podoplanin expression was semi-quantitatively assessed from the percentage of tumor cells with cytoplasmic/membrane staining: 0, no staining; +, <10%; + +, 10–50%; and + + +, >50%.

Results

Immunohistochemical analysis of podoplanin in CNS GCTs

The immunohistochemical findings are summarized in Table 1. Podoplanin immunoreactivity was detected in 26 of 27 (96%) pure germinomas; the staining was graded as + + + in 25 cases and as + in one. One germinoma was negative for podoplanin. Including germinomatous components in mixed GCTs, 40 of 41 (98%) germinomas were stained by YM-1.

Immunostaining for podoplanin showed a diffuse cell-surface pattern in germinoma cells (Fig. 1a). Immunostaining revealed germinoma cells infiltrating into brain parenchyma (Fig. 1b) and in the germinomatous components of mixed tumors (Fig. 1c). Nontumor components such as infiltrated lymphocytes and stromal cells were negative for podoplanin, as were STGCs.

Among the non-germinomatous GCTs and mixed GCTs, 12 of 17 immature teratomas were positive for
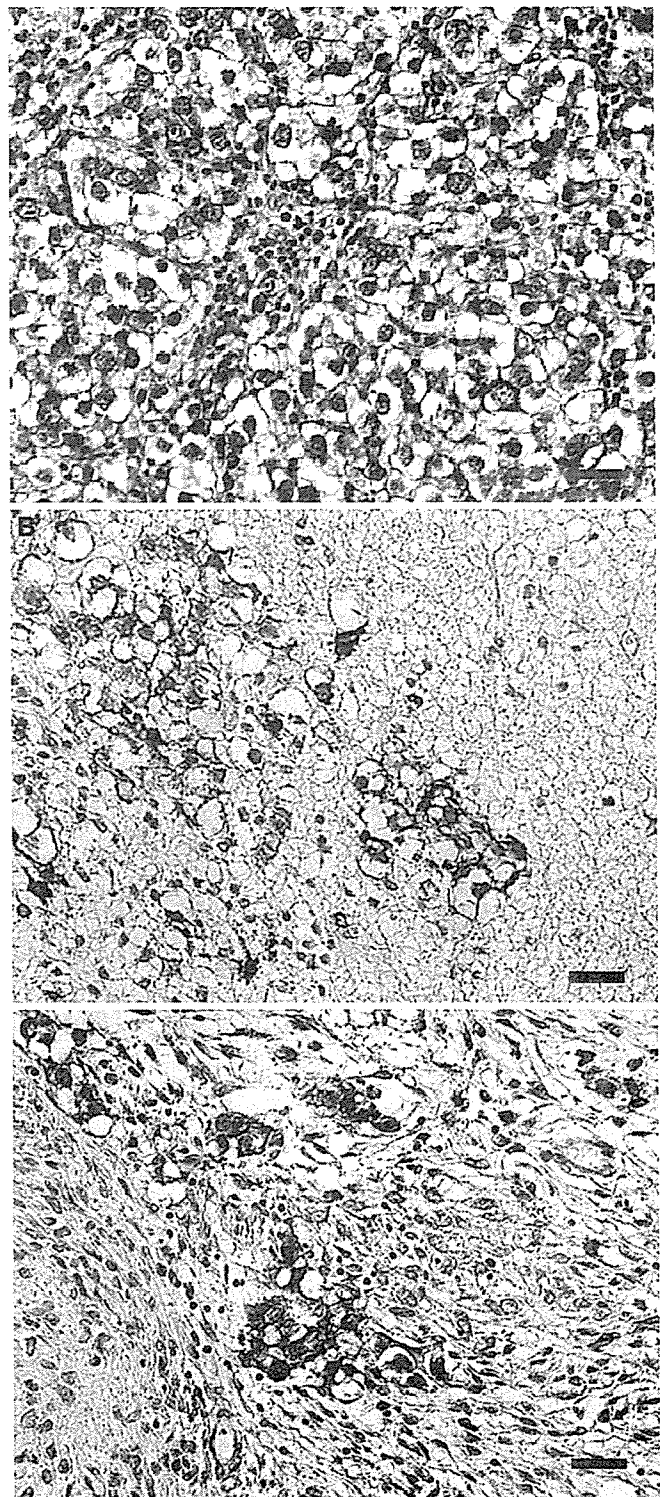
Fig. 1 Immunohistochemical detection of podoplanin in CNS germinomas. a The surface of germinoma cells is strongly positive (*brownish color*). Lymphocytes and interstitial cells are negative. Germinoma cells infiltrating into brain parenchyma (b) and germinomatous components in mixed GCTs (c) are also positive. *Bar* 10 μm

podoplanin; in all cases, the staining was focal (+) and limited to basal layers of immature squamous epithelium and immature columnar epithelium (Fig. 2a, b). Seven

embryonal carcinomas, seven choriocarcinomas, and seven yolk sac tumors were not stained with YM-1 (Fig. 2c–e, Table 1).

In pineal region, GCTs need to be distinguished from other tumors (e.g., metastatic brain tumors, pineocytomas, and pineoblastomas). Therefore, we examined the expression of podoplanin in other CNS tumors to assess the specificity of podoplanin in distinguishing germinomas from certain metastatic brain tumors and some primary brain tumors in pineal region. The immunohistochemical findings are summarized in Table 2. Podoplanin immunoreactivity was detected in one of three (33%) metastatic squamous carcinomas of the lung; the staining was graded as +, although none of the adenocarcinomas of the lung were positive for podoplanin ($n=4$). Other metastatic tumors from colorectal cancer ($n=1$), renal cell carcinomas ($n=2$) and breast cancer ($n=3$) did not express podoplanin. Primary brain tumors in pineal region such as CNS lymphoma ($n=10$), pineocytoma ($n=3$), pineoblastoma ($n=3$), and meningioma ($n=4$) were negative for podoplanin. Other

primary brain tumors such as central neurocytoma ($n=3$) and schwannoma ($n=3$) were also negative.

To confirm the immunohistochemical findings from CNS GCTs, lysates of frozen tumor specimens from seven patients were analyzed by western-blot analysis (Fig. 3). Podoplanin protein was overexpressed in germinoma, but not in choriocarcinoma, yolk sac tumor or normal brain tissue. Podoplanin was also detected in two immature teratomas and one mixed tumor containing immature teratoma, germinoma, and embryonal carcinoma.

Discussion

In this study of 62 primary GCTs of the CNS, immunostaining with monoclonal antibody YM-1 demonstrated podoplanin immunoreactivity in 98% (40/41) of pure or mixed germinomas and a limited number of immature teratomas, but not in embryonal carcinoma, yolk sac tumor, choriocarcinoma, or teratoma. In mixed

Fig. 2 Photomicrographs showing immunohistochemical detection of podoplanin in nongerminomatous GCTs. In immature teratomas, positive staining for podoplanin (*brownish color*) is limited to basal layers of immature squamous epithelium (**a**) and immature columnar epithelial cells (**b**). Embryonal carcinoma (**c**), yolk sac tumor (**d**), and choriocarcinoma (**e**) are negative for podoplanin. *Bar* 10 μm
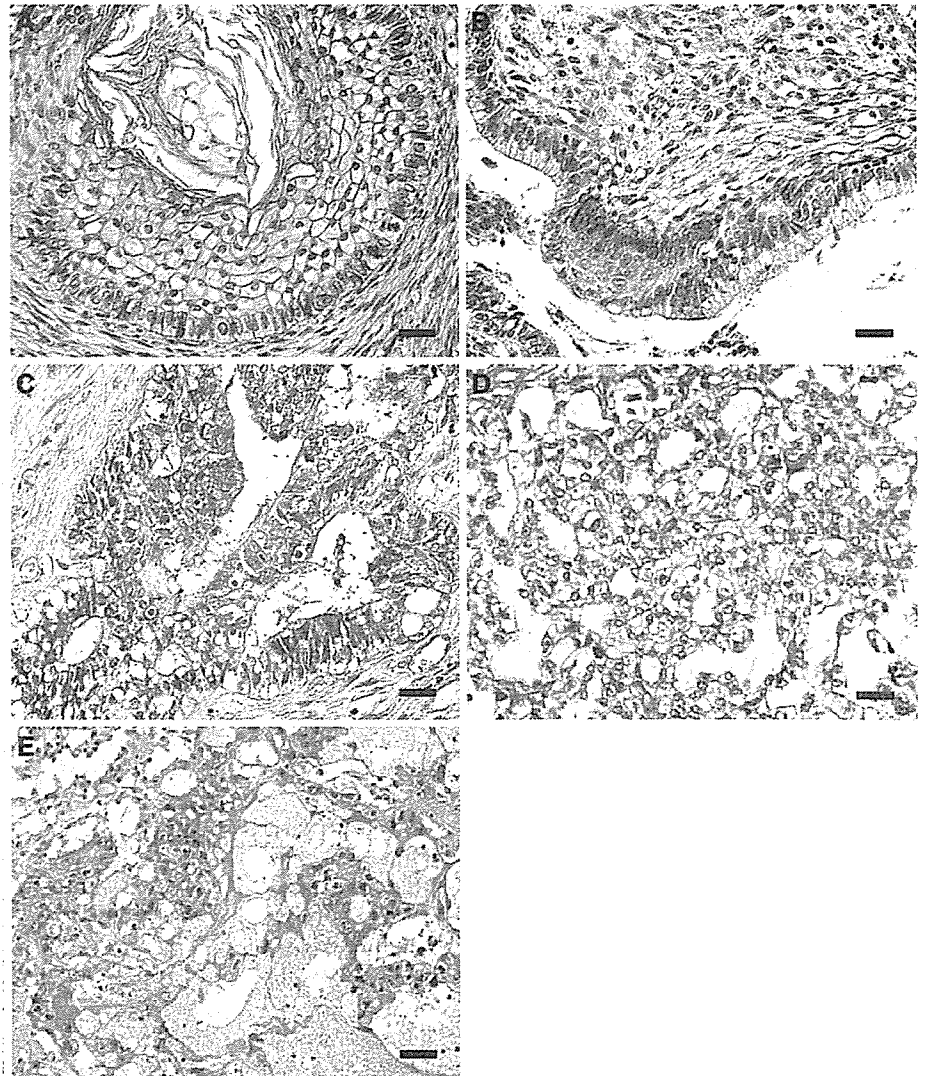
Table 2 Results of podoplanin immunostaining in patients with metastatic brain tumors and primary brain tumors

Tumor type	No. of cases	Podoplanin immunostaining			
		+++	++	+	−
Matastatic brain tumors					
Lung					
Adenocarcinoma	4	0	0	0	4
Sqamous cell carcinoma	3	0	0	1	2
Breast	3	0	0	0	3
Renal cell	2	0	0	0	2
Colorectal	1	0	0	0	1
Primary brain tumors					
Lymphoma	10	0	0	0	10
Pineocytoma	3	0	0	0	3
Pineoblastoma	3	0	0	0	3
Meningioma	4	0	0	0	4
Central neurocytoma	3	0	0	0	3
Schwannoma	3	0	0	0	3
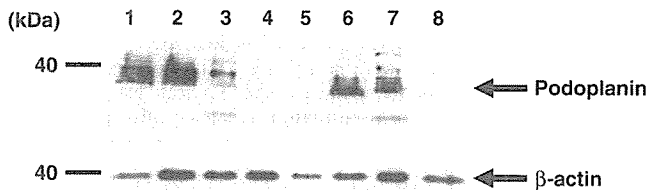
Fig. 3 Western-blot analysis of podoplanin expression in CNS GCTs. Tumor tissues from a germinoma (*lanes 1* and *2*), a mixed tumor (mainly embryonal carcinoma with immature teratoma/germinoma) (*lane 3*), an embryonal carcinoma (*lane 4*), a yolk sac tumor (*lane 5*), an immature teratoma (*lanes 6* and *7*), and normal brain (*lane 8*) were solubilized and immunoblotted with anti-human podoplanin monoclonal antibody YM-1 (*upper panel*) or anti-β-actin antibody (*lower panel*)

GCTs, staining for podoplanin was restricted to germinomatous and immature teratoma components and highlighted germinoma cells. These findings suggest that podoplanin may be a sensitive immunohistochemical marker of CNS germinoma.

Distinguishing germinoma from non-germinomatous GCTs is of paramount importance in patient management. Neuroradiologic findings are not particularly helpful for differentiating between histological subtypes of GCTs [12]. Unlike testicular GCTs, diagnosis of CNS GCTs often requires immunohistochemical analysis because of the small size of the biopsy samples by recent less invasive surgery and the morbidity associated with irradiation of the brain. In addition, a granulomatous inflammatory reaction sometimes overwhelms the tumor cell parenchyma, causing a diagnostic failure at biopsy [8]. Therefore, a specific immunohistochemical marker would be extremely useful for identifying tumor cells in biopsy samples submitted for diagnosis.

Antibodies to PLAP, a cell-surface glycoprotein elaborated by syncytiotrophoblasts and produced by primordial germ cells, have been widely used for immu-

nochemical diagnosis of germinomas and seminomas. About 75–100% of germinomas and 33–86% of non-germinomatous GCTs such as embryonal carcinomas are positive for PLAP [21]. Unfortunately, it lacks specificity and its low secretion titer makes detection difficult.

On the other hand, our findings suggest that podoplanin is highly expressed in germinomas and focally in immature teratomas but not in embryonal carcinomas, choriocarcinomas, and yolk sac tumors and any of these components in mixed GCTs. Indeed, the subtypes of nongerminomatous GCTs (e.g., embryonal carcinoma, yolk sac tumor, and choriocarcinoma) occur rarely as a pure form and are mostly seen as a part of a mixed germ cell tumor in CNS GCTs, therefore the number of non-germinomatous GCTs examined in this study might be small to conclude the specificity of podoplanin expression for germinoma.

The most common site of origin for pineal region metastasis is the lung, followed by the breast. In our study, metastatic brain tumors from lung squamous carcinomas occasionally expressed podoplanin, as the primary lung squamous cell carcinoma expressed podoplanin/aggrus [7]. However, adenocarcinomas from lung and other metastatic brain tumors from colorectal cancer, renal cell carcinoma and breast cancer did not express podoplanin. Other primary brain tumors such as CNS lymphoma, pineocytoma, pineoblastoma, meningioma, central neurocytoma, and schwannoma were also negative for podoplanin. Recently, podoplanin was reported to be expressed in hemangioblastoma in the brain [15]. Thus, podoplanin is not a specific marker of germinoma in brain tumors, but could be a useful diagnostic marker for germinomas in CNS GCTs. We suggest that the combination of several markers, such as podoplanin detected by D2-40 or YM-1, PLAP, beta-HCG, and AFP, provides more precise diagnostic information. Establishing the clinical efficacy of podoplanin as a marker for GSTs will require further investigation.

The biological function of podoplanin is largely unknown. In mice, deficiency in T1α/podoplanin causes defects attributed to disruption of epithelial-mesenchymal signaling [13] and to impairments in cell to substratum adhesion and cell migration [16]. In vascular endothelial cells, overexpression of T1α/podoplanin induces elongated cell extensions and significantly increases cell adhesion, migration, and tube formation by promoting rearrangement of the actin cytoskeleton [16]. PA2.26 antigen/podoplanin was identified as a cell-surface protein induced in epidermal carcinogenesis and skin remodeling. Expression of PA2.26 antigen/podoplanin in pre-malignant keratinocytes induces fully transformed and metastatic phenotype [18, 19]. Human PA2.26 antigen/podoplanin has been found in the invasive front of oral squamous cell carcinomas, consistent with a role in tumor cell migration and invasion [10]. Although germinomas rarely metastasize outside the CNS, they have a predilection for disseminating within the subarachnoid space and for invading sur-

rounding brain tissue [1, 3, 23]. These findings, together with the upregulated expression of podoplanin we observed in CNS germinomas, suggest a potential role of podoplanin in the progression, invasion, and dissemination of CNS germinoma; however, its direct biological function in germinomas remains to be established. We are currently investigating whether enhanced podoplanin expression contributes to the invasive spread of experimental tumors.

In conclusion, podoplanin appears to be a sensitive marker of germinoma and thus may be useful for diagnosis and for monitoring the effects of treatment. Because of its oncogenic potential, high-level expression in germinomas, and localization on the cell surface, podoplanin is a potential target for antibody-based therapy.

References

1. Balmaceda C, Modak S, Finlay J (1998) Central nervous system germ cell tumors. Semin Oncol 25:243–250
2. Breiteneder-Geleff S, Soleiman A, Kowalski H, Horvat R, Amann G, Kriehuber E, Diem K, Weninger W, Tschachler E, Alitalo K, Kerjaschki D (1999) Angiosarcomas express mixed endothelial phenotypes of blood and lymphatic capillaries: podoplanin as a specific marker for lymphatic endothelium. Am J Pathol 154:385–394
3. Jennings MT, Gelman R, Hochberg F (1985) Intracranial germ-cell tumors: natural history and pathogenesis. J Neurosurg 63:155–167
4. Kaneko M, Kato Y, Kunita A, Fujita N, Tsuruo T, Osawa M (2004) Functional sialylated O-glycan to platelet aggregation on aggrus (T1α/podoplanin) molecules expressed in Chinese hamster ovary cells. J Biol Chem 279:38838–38843
5. Kato Y, Fujita N, Kunita A, Sato S, Kaneko M, Osawa M, Tsuruo T (2003) Molecular identification of aggrus/T1α as a platelet aggregation-inducing factor expressed in colorectal tumors. J Biol Chem 278:51599–51600
6. Kato Y, Sasagawa I, Kaneko M, Osawa M, Fujita N, Tsuruo T (2004) Aggrus: a diagnostic marker that distinguishes seminoma from embryonal carcinoma in testicular germ cell tumors. Oncogene. 23:8552–8556
7. Kato Y, Kaneko M, Sata M, Fujita N, Tsuruo T, Osawa M (2005) Enhanced expression of aggrus (T1α/podoplanin), a platelet-aggregation-inducing factor in lung squamous cell carcinoma. Tumour Biol 26:195–200
8. Kraichoke S, Cosgrove M, Chandrasoma PT (1988) Granulomatous inflammation in pineal germinoma. A cause of diagnostic failure at stereotaxic brain biopsy. Am J Surg Pathol 12:655–660
9. Marks A, Sutherland DR, Bailey D, Iglesias J, Law J, Lei M, Yeger H, Banerjee D, Baumal R (1999) Characterization and distribution of an oncofetal antigen (M2A antigen) expressed on testicular germ cell tumours. Br J Cancer 80:569–578
10. Martin-Villar E, Scholl FG, Gamallo C, Yurrita MM, Munoz-Guerra M, Cruces J, Quintanilla M (2005) Characterization of human PA2.26 antigen (T1α-2, podoplanin), a small membrane mucin induced in oral squamous cell carcinomas. Int J Cancer 113:899–910
11. Matsutani M, Sano K, Takakura K, Fujimaki T, Nakamura O, Funata N, Seto T (1997) Primary intracranial germ cell tumors: a clinical analysis of 153 histologically verified cases. J Neurosurg 86:446–455
12. Matsutani M (2004) Germ cell tumors. In: Berger MS, Prados MD (eds) Textbook of neuro-oncology. Elsevier Saunders, Philadelphia, pp 310–320
13. Ramirez MI, Millien G, Hinds A, Cao YX, Seldin DC, Williams MC (2003) $T1α$, a lung type I cell differentiation gene, is required for normal lung cell proliferation and alveolus formation at birth. Dev Biol 256:61–72
14. Rosenblum MK, Matsutani M, Van Meir EG (2000) CNS Germ cell tumors. In: Kleihues P, Cavenee WK (eds) Pathology and genetics of tumours of the nervous system. International Agency for Research on Cancer Press, Lyons, pp 208–214
15. Roy S, Chu A, Trojanowski JQ, Zhang PJ (2005) D2-40, a novel monoclonal antibody against the M2A antigen as a marker to distinguish hemangioblastomas from renal cell carcinomas. Acta Neuropathol (Berl) 109:497–502
16. Schacht V, Ramirez MI, Hong YK, Hirakawa S, Feng D, Harvey N, Williams M, Dvorak AM, Dvorak HF, Oliver G, Detmar M (2003) T1α/podoplanin deficiency disrupts normal lymphatic vasculature formation and causes lymphedema. EMBO J 22:3546–3556
17. Schacht V, Dadras SS, Johnson LA, Jackson DG, Hong YK, Detmar M (2005) Up-regulation of the lymphatic marker podoplanin, a mucin-type transmembrane glycoprotein, in human squamous cell carcinomas and germ cell tumors. Am J Pathol 166:913–921
18. Scholl FG, Gamallo C, Vilar S, Quintanilla M (1999) Identification of PA2.26 antigen as a novel cell-surface mucin-type glycoprotein that induces plasma membrane extensions and increased motility in keratinocytes. J Cell Sci 112:4601–4613
19. Scholl FG, Gamallo C, Quintanilla M (2000) Ectopic expression of PA2.26 antigen in epidermal keratinocytes leads to destabilization of adherens junctions and malignant progression. Lab Invest 80:1749–1759
20. Sugimoto Y, Watanabe M, Oh-hara T, Sato S, Isoe T, Tsuruo T (1991) Suppression of experimental lung colonization of a metastatic variant of murine colon adenocarcinoma 26 by a monoclonal antibody 8F11 inhibiting tumor cell-induced platelet aggregation. Cancer Res 51:921–925
21. Tada M (1998) Tumor markers. In: Sawamura Y, Shirato H, de Tribolet N (eds) Intracranial germ cell tumors. Springer, Wien, pp 146–153
22. Watanabe M, Okochi E, Sugimoto Y, Tsuruo T (1988) Identification of a platelet-aggregating factor of murine colon adenocarcinoma 26: Mr 44,000 membrane protein as determined by monoclonal antibodies. Cancer Res 48:6411–6416
23. Yoshida K, Sawamura Y (1998) Clinical findings and diagnosis, ophthalmological manifestations In: Sawamura Y, Shirato H, de Tribolet N (eds) Intracranial germ cell tumors. Springer, Vienna, pp 137–145

Stereotactic Radiosurgery Plus Whole-Brain Radiation Therapy vs Stereotactic Radiosurgery Alone for Treatment of Brain Metastases
A Randomized Controlled Trial

Hidefumi Aoyama, MD, PhD

Hiroki Shirato, MD, PhD

Masao Tago, MD, PhD

Keiichi Nakagawa, MD, PhD

Tatsuya Toyoda, MD, PhD

Kazuo Hatano, MD, PhD

Masahiro Kenjyo, MD, PhD

Natsuo Oya, MD, PhD

Saeko Hirota, MD, PhD

Hiroki Shioura, MD, PhD

Etsuo Kunieda, MD, PhD

Taisuke Inomata, MD, PhD

Kazushige Hayakawa, MD, PhD

Norio Katoh, MD

Gen Kobashi, MD, PhD

Context In patients with brain metastases, it is unclear whether adding up-front whole-brain radiation therapy (WBRT) to stereotactic radiosurgery (SRS) has beneficial effects on mortality or neurologic function compared with SRS alone.

Objective To determine if WBRT combined with SRS results in improvements in survival, brain tumor control, functional preservation rate, and frequency of neurologic death.

Design, Setting, and Patients Randomized controlled trial of 132 patients with 1 to 4 brain metastases, each less than 3 cm in diameter, enrolled at 11 hospitals in Japan between October 1999 and December 2003.

Interventions Patients were randomly assigned to receive WBRT plus SRS (65 patients) or SRS alone (67 patients).

Main Outcome Measures The primary end point was overall survival; secondary end points were brain tumor recurrence, salvage brain treatment, functional preservation, toxic effects of radiation, and cause of death.

Results The median survival time and the 1-year actuarial survival rate were 7.5 months and 38.5% (95% confidence interval, 26.7%-50.3%) in the WBRT + SRS group and 8.0 months and 28.4% (95% confidence interval, 17.6%-39.2%) for SRS alone ($P = .42$). The 12-month brain tumor recurrence rate was 46.8% in the WBRT + SRS group and 76.4% for SRS alone group ($P < .001$). Salvage brain treatment was less frequently required in the WBRT + SRS group (n = 10) than with SRS alone (n = 29) ($P < .001$). Death was attributed to neurologic causes in 22.8% of patients in the WBRT + SRS group and in 19.3% of those treated with SRS alone ($P = .64$). There were no significant differences in systemic and neurologic functional preservation and toxic effects of radiation.

Conclusions Compared with SRS alone, the use of WBRT plus SRS did not improve survival for patients with 1 to 4 brain metastases, but intracranial relapse occurred considerably more frequently in those who did not receive WBRT. Consequently, salvage treatment is frequently required when up-front WBRT is not used.

Trial Registration umin.ac.jp/ctr Identifier: C000000412

JAMA. 2006;295:2483-2491   www.jama.com

BRAIN METASTASES OCCUR IN 20% to 40% of all patients with cancer and are generally associated with a poor prognosis.[1,2] The most common route of metastatic dissemination resulting in brain metastases is hematogenous, and it is therefore presumed that the entire brain is "seeded" with micrometastatic disease, even when only a single intracranial lesion is detected. Consequently, whole-brain radiation therapy (WBRT) has been a mainstay of treatment.[1,2]

Recently, the assumption that the entire brain is seeded with micrometastases in all patients with overt brain metastases has been questioned, prompting

For editorial comment see p 2535.

Author Affiliations: Departments of Radiology (Drs Aoyama, Shirato, and Katoh) and Global Health and Epidemiology, Division of Preventive Medicine (Dr Kobashi), Hokkaido University Graduate School of Medicine, Sapporo, Japan; Department of Radiology, University of Tokyo Hospital, Tokyo, Japan (Drs Tago and Nakagawa); Department of Radiology, Kanto Medical Center NTT EC, Tokyo, Japan (Dr Toyoda); Department of Radiology, Chiba Cancer Center, Chiba, Japan (Dr Hatano); Department of Radiology, Hiroshima University School of Medicine, Hiroshima, Japan (Dr Kenjyo); Department of Radiology, Kyoto University School of Medicine, Kyoto, Japan (Dr Oya);

Department of Radiology, Hyogo Medical Center for Adults, Akashi, Japan (Dr Hirota); Department of Radiology, Izumisano General Hospital, Izumisano, Japan (Dr Shioura); Department of Radiology, Keio University School of Medicine, Tokyo, Japan (Dr Kunieda); Department of Radiology, Osaka Medical College, Osaka, Japan (Dr Inomata); Department of Radiology, Kitazato Medical School, Sagamihara, Japan (Dr Hayakawa).

Corresponding Author: Hidefumi Aoyama, MD, PhD, Department of Radiology, Hokkaido University Graduate School of Medicine, North 15, West 7, Kita-ku, Sapporo 060-8638, Japan (h-aoyama@umin.ac.jp).

a contrarian philosophy that in some patients, the intracranial disease is truly limited—the so-called oligometastases situation. For patients who truly have limited intracranial disease, the potential exists that WBRT could be replaced by focal therapeutic options such as resection or stereotactic radiosurgery (SRS), which delivers high-dose, focal radiation.[1-4]

The adverse effects of WBRT require a further examination of its role. Acute adverse effects are generally limited in severity and duration; however, the long-term risks of serious and permanent toxic effects, including cognitive deterioration and cerebellar dysfunction, are poorly understood.[5,6] In the attempt to minimize potential long-term morbidity following WBRT, treatments initially relying on focal therapeutic options are being used with increasing frequency. Although there have been several retrospective reports,[7-14] only 1 prospective randomized study compared the outcome of conventional surgery alone and surgery followed by WBRT.[6] Sneed et al[7] collected raw data on 983 patients from 10 institutions and suggested that there was no survival difference between patients treated with SRS alone and those treated with WBRT plus SRS. Flickinger et al[8] reviewed 116 patients with solitary brain metastases who underwent SRS with or without fractionated large-field radiotherapy and found improved local control, but not improved survival, with the addition of fractionated large-field radiotherapy. Regine et al[9] suggested that SRS alone is associated with an increasingly significant risk of brain tumor recurrence and neurologic deficit with increasing survival time. Pirzkall et al[10] showed a trend for superior local control and survival when SRS was combined with WBRT in 236 patients with 311 brain metastases. Aoyama et al,[11] Chidel et al,[12] and Shirato et al[13] have all shown that omission of WBRT from initial management was not detrimental in terms of overall survival, but brain tumors recurred in more

than 50% of patients treated in this manner. Patchell et al[6] have shown that patients with cancer and single metastases to the brain who receive treatment with surgical resection and postoperative WBRT have fewer recurrences of cancer in the brain and are less likely to die of neurologic causes than are similar patients treated with surgical resection alone.

Herein, we report the results of a prospective, multi-institutional, randomized controlled trial comparing WBRT plus SRS vs SRS alone for patients with limited (defined as ≤4) brain metastases. Through a literature search and examination of clinical trial registries, we confirmed that this is the first multi-institutional, prospective, randomized comparison of WBRT plus SRS vs SRS alone.

METHODS
Eligibility Criteria
Patients were eligible who were aged 18 years or older with 1 to 4 brain metastases, each with a maximum diameter of no more than 3 cm on contrast-enhanced magnetic resonance imaging (MRI) scans, derived from a histologically confirmed systemic cancer. Patients with metastases from small cell carcinoma, lymphoma, germinoma, and multiple myeloma were excluded. Eligible patients had a Karnofsky Performance Status (KPS) score of 70 or higher. The protocol was approved by the institutional review boards of Hokkaido University, Sapporo, Japan, and of 10 other institutions that participated in the trial through the Japanese Radiation Oncology Study Group (JROSG 99-1). Written informed consent was obtained from each patient before entry into the study.

Randomization and Treatment
Randomization was performed at the Hokkaido University Hospital Data Center. A permuted-blocks randomization algorithm was used with a block size of 4. A randomization sheet was created for each institution. After written informed consent was obtained, eligible patients were ran-

domly assigned to receive either up-front WBRT combined with SRS or SRS without up-front WBRT. Prior to randomization, the patients were stratified based on number of brain metastases (single vs 2-4), extent of extracranial disease (active vs stable), and primary tumor site (lung vs other sites). Extracranial disease was considered to be stable when the tumor had been clinically controlled for 6 months or longer prior to the detection of brain metastases.

The WBRT dosage schedule was 30 Gy in 10 fractions over 2 to 2.5 weeks. The WBRT treatment visit proceeded to SRS when patients were assigned to the WBRT + SRS group. The SRS dose was prescribed to the tumor margin. Metastases with a maximum diameter of up to 2 cm were treated with doses of 22 to 25 Gy and those larger than 2 cm were treated with doses of 18 to 20 Gy. The dose was reduced by 30% when the treatment was combined with WBRT because the optimal combination of WBRT and SRS had not been studied in well-conducted, prospective, phase 1 dose escalation trials. In the 1990s, the Radiation Therapy Oncology Group (RTOG) initiated a phase 1 dose escalation trial of SRS alone in patients who had previously undergone radiation treatment.[14] This trial was stopped early without reaching the maximum tolerance dose, and tumor size–dependent dose recommendations for SRS alone were described. No phase 1 trial has ever tested the combination of WBRT and SRS doses. Therefore, there is no well-known or scientifically recommended dose for the combination of WBRT and SRS. There are clearly concerns that the combination could be potentially deleterious. Therefore, various studies have adopted different approaches for selection of the dose combinations to be tested. Several retrospective data suggested that the RTOG dose guidelines might be associated with a higher frequency of late radiation toxic effects when used with WBRT.[10,15] Our preexisting experience of SRS with a 30% reduced SRS dose

combined with WBRT indicated that there is not a significant difference in local tumor control (data not shown) compared with SRS with the dose suggested in the RTOG protocol. Therefore, we decided to use a 30% reduced SRS dose in the WBRT + SRS group in this study.

Follow-up Protocol

We performed clinical evaluations and MRI scans 1 and 3 months after treatment and every 3 months thereafter. In cases in which a recurrence was detected, further treatment was administered at the discretion of the attending physician. The size of the treated lesions was measured in 3 dimensions, and this size, the development of new brain metastases, and the development of leukoencephalopathy associated with radiological findings (according to the National Cancer Institute's Common Toxicity Criteria version 2.0[16]) were scored based on serial MRI scans. Local tumor progression was defined as a radiographic increase of 25% or more in the size of a metastatic lesion (bidimensional product). If an MRI result showed central or heterogeneous low intensity and if the lesion size decreased on serial studies, brain necrosis was scored; positron emission tomography or surgical resection was encouraged as appropriate to confirm MRI findings.

At each visit, functional status and neurologic toxic effects were scored. Systemic functional status was evaluated by using the KPS score. Neurologic function was evaluated according to the criteria listed in TABLE 1.[17] Neurosurgeons or radiation oncologists specializing in neuro-oncology measured the neurologic status as well as the KPS score at the clinic. We did not attempt to blind the investigators with regard to patients' treatment assignments. Systematic functional status and neurologic function were scored by the physicians who treated the patients. An acute toxic effect was identified as an event that arose within 90 days of the initiation of radiotherapy and a late toxic effect was considered as an event that occurred

thereafter, according to the central nervous system toxicity criteria listed among the RTOG Late Radiation Morbidity Scoring Criteria.[18] For all patients who died, the cause of death was determined. The cause of death was determined by autopsy in 1 patient and by clinical evaluation based on the definition proposed by Patchell et al[6] in all other patients. Patients were considered to have died of neurologic causes if they had stable systemic disease and

Table 1. Baseline Characteristics*

Characteristics	WBRT + SRS (n = 65)	SRS Alone (n = 67)
Age at diagnosis, mean (range), y	62.5 (36-78)	62.1 (33-86)
<65	32 (49)	34 (51)
≥65	33 (51)	33 (49)
Men	46 (71)	53 (79)
No. of brain metastases		
1	31 (48)	33 (49)
2-4	34 (52)	34 (51)
Primary tumor site		
Breast	6 (9)	3 (4)
Lung	43 (66)	45 (67)
Colorectal	5 (8)	6 (9)
Kidney	5 (8)	5 (7)
Other	6 (9)	8 (12)
Primary tumor status		
Stable	30 (46)	33 (49)
Active	35 (54)	34 (51)
Extracranial metastases		
Stable	41 (63)	38 (57)
Active	24 (37)	29 (43)
RPA		
Class 1 (aged <65 years; no active extracranial disease)	11 (17)	8 (12)
Class 2 (aged ≥65 years; active extracranial disease)	54 (83)	59 (88)
Histological status		
Squamous cell	11 (17)	11 (16)
Adenocarcinoma	43 (66)	43 (64)
Large cell	2 (3)	4 (6)
Other	9 (14)	9 (13)
KPS score†		
70-80	31 (48)	23 (34)
90-100	34 (52)	44 (66)
Neurologic function		
No symptoms (grade 0)	38 (59)	47 (70)
Minor symptoms, fully active without assistance (grade 1)	12 (18)	13 (19)
Moderate symptoms; fully active but requires assistance (grade 2)	8 (12)	4 (6)
Moderate symptoms; less than fully active, requires assistance (grade 3)	7 (11)	3 (5)
Severe symptoms; totally inactive (grade 4)	0	0
Chemotherapy after brain treatment	18 (38)	19 (40)
Maximum diameter of brain metastases, cm		
Mean (SD)	1.53 (0.78)	1.42 (0.79)
Median (range)	1.40 (0.2-3.0)	1.30 (0.2-3.0)
SRS dose at the tumor margin, mean (SD), Gy	16.6 (3.6)	21.9 (2.7)

Abbreviations: KPS, Karnofsky Performance Status; RPA, recursive partition analysis; SRS, stereotactic radiosurgery; WBRT, whole-brain radiation therapy.
*Data are expressed as No. (%) of participants unless otherwise noted.
†A higher score indicates better performance.

progressive neurologic dysfunction. Patients with severe neurologic disability who died of intercurrent illness were also included among neurologic deaths, as were patients with both rapidly progressive systemic disease and advancing neurologic dysfunction, because these patients also represent brain treatment failures.

Figure 1. Flow of Study Participants

SRS indicates stereotactic radiosurgery; WBRT, whole-brain radiation therapy.

End Points and Statistical Analysis

The primary end point of the study was overall survival. Secondary end points were cause of death, functional preservation, brain tumor recurrence, salvage treatment, and toxic effects of radiation. All analyses were conducted on an intention-to-treat basis. The study was designed to have 80% power to detect an absolute difference of 30% in the median survival time, with a 2-sided α level of .05. Using an estimated median survival time of 8.7 months for the group receiving SRS alone[11] and a follow-up time of 15 months, the sample size required to detect this difference was 89 patients per group. An interim analysis was planned wherein 50 patients would be assigned to each group to determine whether the sample size was large enough to show a significant difference with a 2-sided α level of .05. End points were measured beginning at the date of randomization. Univariate analyses were carried out by the Kaplan-Meier method.[19] We assumed that the survival rate was always higher in the WBRT + SRS group than in the SRS-alone group based on the suggestions in a retrospective study, and we used the log-rank test to compare differences between the groups. The χ^2 test was used to determine the

relationship between 2 categorical variables, and the Fisher exact test was used when small cell sizes were encountered in 2×2 contingency tables. A 2-tailed t test was used to compare the means of continuous variables between the treatment groups. Multivariate analyses were performed to evaluate the factors selected via the univariate analyses ($P<.10$). Stratification in the randomization was taken into account in the statistical analysis. The Cox proportional hazards model was used to calculate hazard ratios and 95% confidence intervals (CIs).[20] A 2-sided P value of .05 or less was considered to reflect statistical significance. Additional covariates were examined as appropriate and are noted in the "Results" section. All statistical analyses were initially performed by a physician (H.A.) using a commercial statistical software package (StatView version 5.0], SAS Institute Inc, Cary, NC), and all results were verified by a statistician (G.K.) using a different software package (SAS, version 9.1, SAS Institute Japan Ltd, Tokyo, Japan).
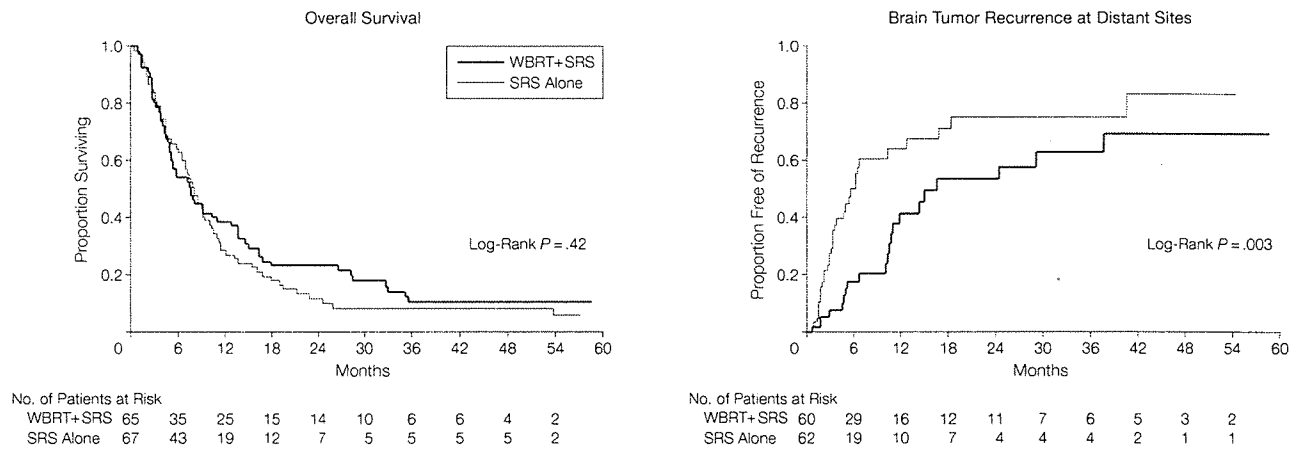
RESULTS

Patients and Treatment

The recruitment period was from October 1999 to December 2003. There were
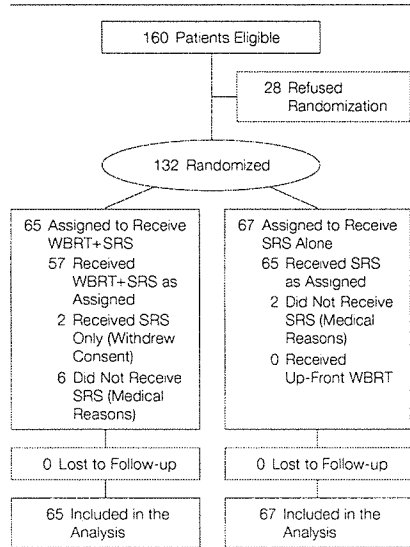
Figure 2. Overall Survival and Brain Tumor Recurrence at Distant Sites

The mean survival time was 7.5 months for patients receiving whole-brain radiation therapy (WBRT) plus stereotactic radiosurgery (SRS) and 8.0 months for patients receiving SRS alone. This difference was not significant (P=.42). There was a statistically significant decrease in brain tumor recurrence in the WBRT+SRS group (P=.003).

160 eligible patients, of whom 132 (83%) were randomized (65 to WBRT + SRS and 67 to SRS alone) (FIGURE 1). The date of last follow-up was April 2005. The interim analysis was performed with 122 patients (about 60 in each group), which takes into account the possible number of patients with protocol violations. Patient accrual was terminated before the planned final accrual number had been reached because the results of the interim analyses indicated that at least 805 patients were necessary to detect a significant difference in the primary end points. In addition, the numbers of patients appeared sufficient to detect a significant difference in brain tumor recurrence rates: 31 patients in each group were shown to be enough to detect a 30% difference in the median month of 50% brain tumor recurrence (16.2 months with WBRT + SRS vs 5.5 months with SRS alone).

There was no statistical difference between the groups in the baseline characteristics of the patients.(Table 1). The median follow-up time was 7.8 months (range, 0.5-58.7 months) for the entire study and 49.2 months (range, 19.6-58.7 months) for survivors. Ninety-two percent of the patients included in the study completed the assigned treatment (Figure 1).

Survival and Cause of Death

By the time of the last follow-up visit in April 2005, 57 patients in the WBRT + SRS group and 62 patients in the SRS-alone group had died. Death was attributed to neurologic causes in 13 patients (22.8%) in the WBRT + SRS group and in 12 patients (19.3%) in the SRS-alone group ($\chi^2 = 0.21$; $P = .64$). The median survival time was 7.5 months with WBRT + SRS and 8.0 months with SRS alone. The higher median survival time with SRS alone was discordant with the 1-year actuarial survival rates of 38.5% (95% CI, 26.7%-50.3%) for the WBRT + SRS group and 28.4% (95% CI, 17.6%-39.2%) for the SRS-alone group ($P = .42$). FIGURE 2A shows that this discor-

dance was due to the crossing of the 2 survival curves. The results of the univariate and multivariate analyses are shown in TABLE 2 and TABLE 3. The number of patients in each institution was too small to allow for a meaningful comparison among institutions. Recursive partition analysis was not included in the multivariate analysis because it is not indepen-

dent of age and extracranial metastases. Treatment group was not found to be significant in either analysis.

Posttreatment Neurologic Toxicity

A summary of posttreatment neurologic toxicity is given in TABLE 4. Symptomatic acute neurologic toxicity was observed in 4 patients receiving WBRT + SRS and in 8 patients receiv-

Table 2. Univariate Survival Analysis

	No. of Participants	Survival Time, Median (Range), mo	P Value
Treatment group			
WBRT + SRS	65	7.5 (0.8-58.7) ⎤	.42
SRS alone	67	8.0 (0.5-57.0) ⎦	
Age, y			
<65	66	8.9 (0.9-58.7) ⎤	.07
≥65	66	6.5 (0.5-55.6) ⎦	
Sex			
Male	99	7.1 (0.5-58.7) ⎤	.20
Female	33	10.5 (0.8-57.0) ⎦	
No. of brain metastases			
1	68	8.6 (1.4-58.7) ⎤	.02
2-4	64	7.3 (0.5-55.6) ⎦	
Primary tumor site			
Lung	88	8.1 (0.5-58.7) ⎤	.33
Other	44	7.1 (0.9-57.0) ⎦	
Primary tumor status			
Stable	69	9.2 (0.9-58.7) ⎤	<.001
Active	63	6.5 (0.5-53.8) ⎦	
Extracranial metastases			
Stable	79	13.3 (1.1-58.7) ⎤	<.001
Active	53	6.1 (0.5-55.6) ⎦	
RPA			
Class 1	19	16.0 (0.9-58.7) ⎤	<.001
Class 2	113	7.5 (0.5-55.6) ⎦	
KPS score			
70-80	54	5.0 (0.5-58.7) ⎤	<.001
90-100	78	9.2 (0.8-57.0) ⎦	
Chemotherapy after brain treatment			
Yes	37	10.1 (1.3-53.8) ⎤	.34
No	95	6.8 (0.5-58.7) ⎦	

Abbreviations: KPS, Karnofsky Performance Status; RPA, recursive partition analysis; SRS, stereotactic radiosurgery; WBRT, whole-brain radiation therapy.

Table 3. Multivariate Survival Analysis

Variables*	Hazard Ratio (95% CI)	P Value
Treatment group (WBRT + SRS)	1.37 (0.93-1.98)	.11
Age (<65 y)	1.48 (1.01-2.16)	.04
No. of brain metastases (1)	1.36 (0.94-1.97)	.10
Primary tumor status (stable)	1.62 (1.11-2.36)	.01
Extracranial metastases (stable)	2.35 (1.55-3.55)	<.001
KPS score (90-100)	1.69 (1.16-2.47)	.007

Abbreviations: CI, confidence interval; KPS, Karnofsky Performance Status; SRS, stereotactic radiosurgery; WBRT, whole-brain radiation therapy.
*Referents appear in parentheses.